Adv Comput Math (2020) 46:78
https://doi.org/10.1007/s10444-020-09819-6

Superconvergent gradient recovery for nonlinear Poisson-Nernst-Planck equations with applications to the ion channel problem

Ying Yang[1] · Ming Tang[2] · Chun Liu[3] · Benzhuo Lu[4] · Liuqiang Zhong[2]

Received: 27 December 2019 / Accepted: 16 October 2020 / Published online: 29 October 2020

Abstract

Poisson-Nernst-Planck equations are widely used to describe the electrodiffusion of ions in a solvated biomolecular system. An error estimate in H^1 norm is obtained for a piecewise finite element approximation to the solution of the nonlinear steady-state Poisson-Nernst-Planck equations. Some superconvergence results are also derived by using the gradient recovery technique for the equations. Numerical results are given to validate the theoretical results. It is also numerically illustrated that the gradient recovery technique can be successfully applied to the computation of the practical ion channel problem to improve the efficiency of the external iteration and save CPU time.

Keywords Nonlinear Poisson-Nernst-Planck equations · Steady state · Finite element method · Error estimate · Superconvergent gradient recovery · Ion channel

Mathematics subject classification (2010) 65N30

1 Introduction

Ion channels are a special integral protein on the cell membrane with characteristic of ion selectivity. They are involved in many physiological activities in bodies, such as the release of neurotransmitters, the contraction of muscles, and other more complex learning and memory [21]. Poisson-Nernst-Planck (PNP) equations are an important theoretical model for simulating the permeation mechanism of ion channels.

Communicated by: Long Chen

✉ Liuqiang Zhong
zhong@scnu.edu.cn

Extended author information available on the last page of the article.

Although PNP model is widely applied in ion channel area and has some success in dealing with experimental data, limitations are also recognized in it. For example, it does not include correlations introduced by the finite diameter of ions, and these are of great importance in determining selectivity of channels and the properties of ionic solutions in general [22]. Some modified PNP models are then developed to deal with them. For example, Lu and Zhou [29] improved the PNP equations by the addition of the size effect, which simulates the biomolecular diffusion-reaction processes well. Hyon et al. [23] derived a modified PNP system for the ion channel taking into account the protein (ion channel) structure compared with the primitive PNP model. These modifications in PNP models always produce strong nonlinearity, which brings some difficulties in analysis and computation for these models. Generally speaking, it is difficult to find the analytic solutions for PNP equations. There appears many literatures on numerical methods for PNP equations, including finite difference method, finite volume method, and finite element method. Finite difference method (FDM) and finite volume method (FVM) have the advantages of implementation simplicity and high accuracy respectively and were successfully applied to solving many PNP models (see, e.g., [8, 15] for FDM and [31, 38] for FVM). These methods are based on structured meshes, on which the position of molecular or protein surface is usually not precisely computed and constructed, which leads to a neglect of the continuity conditions on the solution when applied to practical biomolecular problems. Finite element method is suitable for the irregular surface which is conforming to the molecular boundary, the solution of which satisfies the continuity conditions on the molecular surface, hence leading to more accurate results. There are also some research work on the finite element methods (FEM) (see, e.g., [28–30]).

In contrast to amount of work on the simulation of PNP equations, the work of analysis for PNP equations seems limited, especially for finite element method. The existence and uniqueness of the finite element approximation for the time-dependent PNP equations are shown in [33]. Yang and Lu [42] presented an error analysis of the finite element method for a type of steady-state PNP equations modeling the electrodiffusion of ions in a solvated biomolecular system. Sun et al. [36] analyzed a Crank-Nicolson scheme of the finite element method for time-dependent PNP equations, where both an optimal H^1 norm error estimate and a sub-optimal L^2 norm error estimate were derived for the linear finite element approximations. Then Gao and He [17] obtained an optimal L^2 error estimate with linear finite element approximations for a linearized backward Euler scheme, which can preserve mass conservation and energy decay. Recently, Shi and Yang [35] also presented an optimal L^2 norm error estimate for the backward Euler scheme of time-dependent PNP equations. Compared with the work in [17], the backward Euler scheme applied in [35] is nonlinear but a smoother solution is required, since the superconvergence technique is used in the analysis.

In this paper, the finite element method is studied for a kind of generic nonlinear steady-state PNP model (see (15) for detailed description), and many modified PNP models can be viewed as special types of it. The error estimate in H^1 norm is presented for a piecewise finite element approximation to the nonlinear steady-state PNP equations. Based on the derived error estimate, the superconvergence analysis is also studied for the equations by using the gradient recovery technique. This technique can be applied as a post-process to improve the accuracy of gradient of the finite element approximation, the efficiency of which is illustrated by the numerical results for a nonlinear PNP system in Section 5.

We note that gradient recovery technique is one of the effective ways to develop superconvergence for the finite element approximation, which has been used to improve the numerical approximation and supply a posteriori error estimation for the adaptive procedure (see, e.g., [4, 5, 7, 9, 16, 25, 27, 32, 44]). The well-known Superconvergence Patch Recovery (SPR) method was introduced by Zienkiewicz and Zhu [44], which has attracted considerable attention in the community of finite element methods. Zhang and Naga [45] developed the Polynomial Preserving Recovery (PPR) method, which not only maintains the simplicity, efficiency, and superconvergence properties of the SPR method but also is superconvergent for the linear element under the chevon pattern and ultraconvergent at element edge centers for the quadratic element under the regular pattern. Later, some gradient superconvergences are presented and analyzed on three-dimensional mildly structured meshes (cf., e.g., [11] and [12]), which requires less restrictions on the assumption of the meshes. Recently, Gou and Yang [19] proposed a new gradient recovery method for elliptic interface problem using body-fitted meshes, the superconvergence of which holds on both mildly unstructured meshes and adaptive meshes. A superconvergent gradient recovery method for the virtual element method is presented in [20] by performing local post-processing only on the degrees of freedom, which generalizes the idea of PPR to general polygonal meshes.

In this work, we study the superconvergence of the gradient recovery method for the PNP equations. In [43], we presented the superconvergent results for the Poisson Boltzmann equation (PBE), which can be viewed as a special type of PNP equations. Li et al. proposed a new gradient recovery method for PBE in [26], which can preserve the flux-jump on the interface. Compared with PBE considered in [26] and [43], the PNP model is a coupled nonlinear system, and the analysis and implementation of the gradient recovery method are more complex. We also note that the superconvergence analysis in H^1 norm is recently introduced by Shi and Yang [35] for the linear element approximation of the two-dimensional time-dependent PNP equations. Compared with [35], the model considered here is nonlinear steady-state PNP equations, while it is a linear time-dependent one in [35]. Because of the large difference of the model, the arguments used in the error analysis are quite different. Moreover, the gradient recovery technique is applied to a practical ion channel problem to improve the computation efficiency of the external iteration, which is one of the contributions in this paper. Next, we shall introduce the idea of the application of the gradient recovery technique in a simple but informal way.

The PNP equations for the ion channel in Section 6 can be rewritten as the following simpler form:

$$\begin{cases} \nabla \cdot \Big(\alpha^i \nabla p^i + \beta^i p^i \nabla \phi + \gamma^i p^i g(\nabla p^i)\Big) = 0, \quad i = 1, 2, ..., n, \\ -\nabla(\epsilon \nabla \phi) - \lambda \sum_{i=1}^{n} q^i p^i = F, \end{cases} \tag{1}$$

where ϕ and p^i, $i = 1, 2, ..., n$ are unknowns, ϕ is the electrostatic potential, and p^i is the concentration of the ith ion species. The detailed description of the coefficients $\alpha^i, \beta^i, \gamma^i, \epsilon, \lambda, q^i$ and the nonlinear term g can be found in (68) and (69) in Section 6. Suppose the finite element approximation (p_h^i, ϕ_h) for PNP equations (1) is as follows:

$$\begin{cases} (\alpha^i \nabla p_h^i, \nabla v_h) + (\beta^i p_h^i \nabla \phi_h, \nabla v_h) + (\gamma^i p_h^i g(\nabla p_h^i), \nabla v_h) = 0, \ \ \forall v_h \in S^h, \ i = 1, 2, ..., n, \\ (\epsilon \nabla \phi_h, \nabla w_h) - (\lambda \sum_{i=1}^{n} q^i p_h^i, w_h) = (F, w_h), \ \ \forall w_h \in S^h, \end{cases}$$

where S^h is the linear finite element space. The commonly used decoupled method for the above system is the Gummel iteration [18] (or called external iteration in this paper): given the initial value ϕ_h^0, for $k \geq 0$, find $(p_h^{i,k+1}, \phi_h^{k+1})$ such that:

$$\begin{cases} (\alpha^i \nabla p_h^{i,k+1}, \nabla v_h) + (\beta^i p_h^{i,k+1} \nabla \phi_h^k, \nabla v_h) + (\gamma^i p_h^{i,k+1} g(\nabla p_h^{i,k+1}), \nabla v_h) = 0, \ \ \forall v_h \in S^h, \ i = 1, 2, ..., n, \\ (\epsilon \nabla \phi_h^{k+1}, \nabla w_h) - (\lambda \sum_{i=1}^{n} q^i p_h^{i,k+1}, w_h) = (F, w_h), \ \ \forall w_h \in S_0^h. \end{cases}$$

It is known that the gradient approximations $\nabla \phi_h$ and ∇p_h^i are required to computed in each step of the above iteration. Since the superconvergence analysis in Section 4 shows that the accuracy of $\nabla \phi_h$ and ∇p_h^i can be improved by using the gradient recovery technique as a post-process, the gradients after post-processing are better approximations to the true gradients than $\nabla \phi_h$ and ∇p_h^i. Hence, they can be used to replace $\nabla \phi_h$ and ∇p_h^i in every step of the external iteration to improve the efficiency of the iteration. The numerical example for an ion channel problem shows that a lot of CPU time can be saved if the gradient recovery technique is applied to the external iteration for the nonlinear PNP model.

The structure of the paper is as follows. Section 2 mainly introduces the steady-state PNP and nonlinear PNP models. Section 3 presents some finite element error estimates for both PNP and nonlinear PNP equations. Superconvergence results for PNP and nonlinear PNP equations are shown in Section 4. The numerical examples with analytic solutions are reported in Section 5. In Section 6, a numerical experiment for practical ion channel problem is shown. Finally, some concluding remarks are provided.

2 Preliminaries

Let $\Omega \subset R^3$ be a polyhedral convex domain with a Lipschitz-continuous boundary $\partial\Omega$. We shall adopt the standard notations for Sobolev spaces $W^{s,p}(\Omega)$ and their associated norms and semi-norms [1, 6]. For $p = 2$, we denote $H^s(\Omega) = W^{s,2}(\Omega)$ and $H_0^1(\Omega) = \{v | v \in H^1(\Omega) : v \mid_{\partial\Omega} = 0\}$, where $v \mid_{\partial\Omega} = 0$ is in the sense of trace. The space $H^{-1}(\Omega)$ is the dual of $H_0^1(\Omega)$. Let $\| \cdot \|_{s,p,\Omega} = \| \cdot \|_{W^{s,p}(\Omega)}$ and $(\cdot, \cdot)$ be the standard L^2-inner product. For simplicity, $\| \cdot \|_1 = \| \cdot \|_{W^{1,2}(\Omega)}$, $\| \cdot \|_0 = \| \cdot \|_{L^2(\Omega)}$ and $\| \cdot \|_{0,\infty} = \| \cdot \|_{L^\infty(\Omega)}$.

Also let $T_h = \{\tau\}$ consist of shape-regular simplices of Ω with mesh-size function $h(x)$, whose value is the maximum diameter of the elements τ containing x. For similicity, we assume that T_h is uniform.

$$S^h = \{v \in H^1(\Omega) : v|_\tau \in p^1(\tau), \forall \tau \in T_h\}, \quad S_0^h = S^h \cap H_0^1(\Omega), \tag{2}$$

where $p^1(\tau)$ is the space of linear polynomials on τ. Throughout this paper, C denotes a positive constant independent of h but may have different values at different places.

2.1 The steady-state Poisson-Nernst-Planck equations

We consider the following steady-state PNP system:

$$\begin{cases} -\nabla \cdot \left(\nabla p^i + q^i p^i \nabla \phi\right) = F_i, \ \text{ in } \ \Omega, \ i = 1, 2, ..., n, \\ -\nabla \cdot (\nabla \phi) - \sum\limits_{i=1}^{n} q^i p^i = f, \ \text{ in } \ \Omega \subset R^3, \end{cases} \tag{3}$$

with the homogeneous Dirichlet boundary conditions:

$$\begin{cases} \phi = 0, \ \text{ on } \ \partial\Omega, \\ p^i = 0, \ \text{ on } \ \partial\Omega, \end{cases}$$

where p^i is the concentration of the ith species particle with charge q^i (constant), $i = 1, 2, \cdots, n$, ϕ is the electrostatic potential, and F_i and f are the reaction terms.

The weak formulation of (3) reads: find p^i, $i = 1, 2, ..., n$ and $\phi \in H_0^1(\Omega)$ such that:

$$\begin{cases} (\nabla p^i, \nabla v) + (q^i p^i \nabla \phi, \nabla v) = (F_i, v), \ \ \forall v \in H_0^1(\Omega), \ \ i = 1, 2, ..., n, \\ (\nabla \phi, \nabla w) - \sum\limits_{i=1}^{n} (q^i p^i, w) = (f, w), \ \ \forall w \in H_0^1(\Omega). \end{cases} \tag{4}$$

Assume there exists a unique solution (ϕ, p^i) $(i = 1, 2, .., n)$ satisfying (4). The corresponding standard finite element approximation to problem (4) is defined as follows: find p_h^i, $i = 1, 2, ..., n$ and $\phi_h \in S_0^h$ such that

$$\begin{cases} (\nabla p_h^i, \nabla v_h) + (q^i p_h^i \nabla \phi_h, \nabla v_h) = (F_i, v_h), \ \ \forall v_h \in S_0^h, \ \ i = 1, 2, ..., n, \\ (\nabla \phi_h, \nabla w_h) - \sum\limits_{i=1}^{n} q^i (p_h^i, w_h) = (f, w_h), \ \ \forall w_h \in S_0^h. \end{cases} \tag{5}$$

Next, we introduce two lemmas for the interpolant. The first one is the standard estimate for the interpolant and the second one shall be used in the superconvergence analysis.

Lemma 2.1 [6] *If u_I be the nodal linear Lagrange interpolant of $u \in W^{2,p}(\Omega)$, then we have the estimate:*

$$||u - u_I||_{0,p} + h||u - u_I||_{1,p} \leq Ch^2||u||_{2,p}. \tag{6}$$

Lemma 2.2 [3] *If u_I be the nodal linear Lagrange interpolant of $u \in H^3(\Omega)$, then we have the estimate:*

$$(\nabla(u-u_I), \nabla w_h) = O(h^2)|u|_3 \|\nabla w_h\|_0, \quad \forall w_h \in S_0^h. \tag{7}$$

The following lemmas are required to present the error estimates for p_h^i.

Lemma 2.3 *Let (p^i, ϕ) and (p_h^i, ϕ_h) be the solutions to (4) and (5), respectively. If $\phi \in H^3(\Omega)$, then we have:*

$$\|\phi_h - \phi_I\|_1 \le C(h^2 + \sum_{i=1}^{n} \|p^i - p_h^i\|_0). \tag{8}$$

Proof By (4) and (5), for any $w_h \in S_0^h$, we get:

$$\begin{aligned}(\nabla(\phi_h - \phi_I), \nabla w_h) &= (\nabla(\phi_h - \phi), \nabla w_h) + (\nabla(\phi - \phi_I), \nabla w_h)\\ &= \sum_{i=1}^{n} q^i (p_h^i - p^i, w_h) + (\nabla(\phi - \phi_I), \nabla w_h)\\ &\le C(\sum_{i=1}^{n} \|p_h^i - p^i\|_0 \|w_h\|_0 + h^2 \|\phi\|_3 \|\nabla w_h\|_0),\end{aligned}$$

where (7) is also used. Taking $w_h = \phi_h - \phi_I$ and by Poincaré inequality, we can easily obtain the result of Lemma 2.3. □

Lemma 2.4 *Let (p^i, ϕ) and (p_h^i, ϕ_h) be the solutions to (4) and (5), respectively. If $\phi \in W^{2,\infty}(\Omega)$ and $f \in L^4(\Omega)$ then we have:*

$$\|\nabla \phi_h\|_{0,\infty} \le C. \tag{9}$$

Proof From (5), we know ϕ_h is the finite element approximation to the solution of the following problem:

$$-\Delta \widetilde{\phi} = \sum_{i=1}^{n} q^i p_h^i + f.$$

By Gagliardo-Nirenberg-Sobolev inequality and using the regularity result in [14], we get:

$$||\nabla \phi_h||_{0,\infty} \le C||\widetilde{\phi}||_{1,\infty} \le C||\widetilde{\phi}||_{2,4} \le C||\sum_{i=1}^{n} q^i p_h^i + f||_{0,4}.$$

Hence, by using Gagliardo-Nirenberg-Sobolev inequality, we have:

$$||\nabla \phi_h||_{0,\infty} \le C\left(\sum_{i=1}^{n} ||p_h^i||_{0,4} + ||f||_{0,4}\right) \le C\left(\sum_{i=1}^{n} ||p_h^i||_{1,2} + ||f||_{0,4}\right) \le C.$$

Thus, we finish the proof of Lemma 2.4. □

Lemma 2.5 *Let (p^i, ϕ) and (p_h^i, ϕ_h) be the solutions to (4) and (5), respectively. If $\phi \in H^3(\Omega) \cap W^{2,\infty}(\Omega)$, $p^i \in L^\infty(\Omega)$ and $f \in L^4(\Omega)$, then we have:*

$$(p^i \nabla\phi - p_h^i \nabla\phi_h, \nabla v_h) \le C(h^2 + \sum_{i=1}^n \|p^i - p_h^i\|_0)\|\nabla v_h\|_0, \quad \forall v_h \in S_0^h. \tag{10}$$

Proof Note that for any $v_h \in S_0^h$,

$$\begin{aligned}(p^i \nabla\phi - p_h^i \nabla\phi_h, \nabla v_h) &= (p^i(\nabla\phi - \nabla\phi_h), \nabla v_h) + (\nabla\phi_h(p^i - p_h^i), \nabla v_h)\\ &= (p^i(\nabla\phi - \nabla\phi_I), \nabla v_h) + (p^i(\nabla\phi_I - \nabla\phi_h), \nabla v_h) + (\nabla\phi_h(p^i - p_h^i), \nabla v_h)\\ &\le |(p^i(\nabla\phi - \nabla\phi_I), \nabla v_h)| + (\|p^i\|_{0,\infty}\|\nabla\phi_I - \nabla\phi_h\|_0 + \|\nabla\phi_h\|_{0,\infty}\|p^i - p_h^i\|_0)\|\nabla v_h\|_0.\end{aligned}$$

Inserting (8) and (9) into the above inequality and using the assumption $p^i \in L^\infty(\Omega)$, we get:

$$(p^i \nabla\phi - p_h^i \nabla\phi_h, \nabla v_h) \le |(p^i(\nabla\phi - \nabla\phi_I), \nabla v_h)| + C(h^2 + \sum_{i=1}^n \|p^i - p_h^i\|_0)\|\nabla v_h\|_0. \tag{11}$$

Now we turn to estimate $(p^i(\nabla\phi - \nabla\phi_I), \nabla v_h)$. First for any $u \in W^{1,\infty}(\tau)$, $\forall \tau \in T^h$, denote the average of u on the element τ by $\bar{u} = \frac{1}{\tau}\int_\tau u\, dxdydz$. We know that:

$$\|u - \bar{u}\|_{0,\infty,\tau} \le Ch_\tau \|u\|_{1,\infty,\tau}. \tag{12}$$

Then $(p^i(\nabla\phi - \nabla\phi_I), \nabla v_h)$ is divided into two parts as follows:

$$\begin{aligned}(p^i(\nabla\phi - \nabla\phi_I), \nabla v_h) &= \sum_\tau ((p^i - \bar{p^i})(\nabla\phi - \nabla\phi_I), \nabla v_h)_\tau + (\bar{p^i}(\nabla\phi - \nabla\phi_I), \nabla v_h)_\tau\\ &\le \sum_\tau (\|p^i - \bar{p^i}\|_{0,\infty,\tau}\|\nabla\phi - \nabla\phi_I\|_{0,\tau}\|\nabla v_h\|_{0,\tau}) + C((\nabla\phi - \nabla\phi_I), \nabla v_h).\end{aligned} \tag{13}$$

Therefore, by (12) and (7), we get:

$$(p^i(\nabla\phi - \nabla\phi_I), \nabla v_h) \le C(h^2 + \sum_{i=1}^n \|p^i - p_h^i\|_0)\|\nabla v_h\|_0. \tag{14}$$

Applying (14) to (11) then estimate (10) yields. □

2.2 A nonlinear steady-state Poisson-Nernst-Planck model

Consider the following nonlinear Poisson-Nernst-Planck equations:

$$\begin{cases}\mathcal{L}p^i \equiv -\nabla\cdot(\alpha(x, p^i)\nabla p^i + \beta(x, p^i) + \gamma(x, p^i)\nabla\phi) + g(x, p^i) = 0, \ \text{in } \Omega,\ i = 1, 2, \cdots, n,\\ -\nabla\cdot(\nabla\phi) - \sum_{i=1}^n q^i p^i = f, \ \text{in } \Omega.\end{cases} \tag{15}$$

with Dirichlet boundary conditions:

$$\begin{cases}\phi = 0, \ \text{on } \partial\Omega,\\ p^i = 0, \ \text{on } \partial\Omega.\end{cases} \tag{16}$$

We suppose that $\alpha(x, y) : \bar{\Omega} \times R^1 \to R^3 \times R^3$, $\beta(x, y) : \bar{\Omega} \times R^1 \to R^3$, $\gamma(x, y) : \bar{\Omega} \times R^1 \to R^1$, $g(x, y) : \bar{\Omega} \times R^1 \to R^1$ are smooth and the equation (15) has a solution $p^i \in H_0^1(\Omega) \cap W^{1,p}(\Omega)$ and $\phi \in H_0^1(\Omega) \cap W^{2,\infty}(\Omega)$ for some $p > 3$. For any $w \in H_0^1(\Omega)\cap W^{1,p}(\Omega)$ and $\phi \in H_0^1(\Omega)$, the linearized operator $\mathcal{L}$ at p^i(namely, the *Fréchet* derivative of $\mathcal{L}$ at p^i) is given by:

$$\mathcal{L}'(p^i)\varphi = -\nabla\cdot(\alpha(\cdot,p^i)\nabla\varphi + (\alpha_y(\cdot,p^i)\nabla p^i + \beta_y(\cdot,p^i) + \gamma^i(\cdot,p^i)\nabla\phi)\varphi) + g_y(\cdot,p^i)\varphi.$$

Our basic assumptions are, first of all, for the solution p^i of the equation:

$$\xi^T\alpha(x,p^i)\xi \geq C^{-1}|\xi|^2, \qquad \forall\xi\in R^3, \quad x\in\bar{\Omega}, \tag{17}$$

for some constant $C > 0$ and, secondly, $\mathcal{L}'(p^i) : H_0^1(\Omega) \to H^{-1}(\Omega)$ is an isomorphism. As a result of these assumptions, p^i must be an isolated solution. Denote by:

$$A(w,v) = (\alpha(\cdot,w)\nabla w + \beta(\cdot,w),\nabla v) + (g(\cdot,w),v),$$

and

$$B(w,\psi,v) = (\gamma(\cdot,w)\nabla\psi,\nabla v).$$

Then the solution (p^i,ϕ) to (15)–(16) satisfies:

$$A(p^i,v) + B(p^i,\phi,v) = 0, \qquad \forall v\in H_0^1(\Omega), \quad i=1,2,...,n, \tag{18}$$

$$(\nabla\phi,\nabla v) = (\sum_{i=1}^n q^i p^i, v) + (f,v), \quad \forall v\in H_0^1(\Omega). \tag{19}$$

The corresponding standard finite element approximation is to find p_h^i, $i = 1,2,...,n$ and $\phi_h \in S_0^h$ such that:

$$A(p_h^i,v_h) + B(p_h^i,\phi_h,v_h) = 0, \qquad \forall v_h\in S_0^h, \quad i=1,2,...,n, \tag{20}$$

$$(\nabla\phi_h,\nabla v_h) = (\sum_{i=1}^n q^i p_h^i, v_h) + (f,v_h), \quad \forall v_h\in S_0^h. \tag{21}$$

For any $w \in W_0^{1,p}(\Omega)$, introducing the bilinear form:

$$A'(w,\varphi,v) = (\alpha(\cdot,w)\nabla\varphi + (\alpha_y(\cdot,w)\nabla w + \beta_y(\cdot,w))\varphi,\nabla v) + (g_y(\cdot,w)\varphi,v),$$

then we have the following lemma.

Lemma 2.6 [39] *If* $h \ll 1$ *and* p^i *is the solution to (18)-(19), then:*

$$\|w_h\|_1 \leq C \sup_{\varphi\in S_0^h(\Omega)} \frac{A'(p^i,w_h,\varphi)}{\|\varphi\|_1}, \quad \forall w_h\in S_0^h. \tag{22}$$

For any $w,\psi,\chi,\kappa,v \in H_0^1(\Omega)$, define the remainder:

$$R(w,\psi,\chi,\kappa,v) = A(\chi,v) + B(\chi,\kappa,v) - A(w,v) - B(w,\psi,v) - A'(w,\chi-w,v), \tag{23}$$

then we have the following estimates for the remainder which is required in our analysis.

Lemma 2.7 *Let (ϕ, p^i) be the solution to (18)–(19). The functions p_h^i and $\phi_h \in S_0^h$ are solutions to (20) if and only if:*

$$A'(p^i, p^i - p_h^i, v_h) = R(p^i, \phi, p_h^i, \phi_h, v_h), \quad \forall v_h \in S_0^h. \tag{24}$$

Moreover, for any $w, \psi, \chi, v \in H_0^1(\Omega)$, $\psi \in H^3(\Omega)$, the remainder R satisfies:

$$\begin{aligned}|R(w, \psi, \chi, \kappa, v)| \le\ & C_a||v||_1(||w-\chi||_{1,3}||w-\chi||_1 \\ &+ (||\nabla w||_{0,p} + ||\nabla\chi||_{0,p})||w-\chi||_{1,3}||w-\chi||_1 + h^2 \\ &+ ||\nabla\psi_I - \nabla\kappa||_0 + ||\nabla\kappa||_{0,\infty}||\gamma(\cdot,\chi) - \gamma(\cdot, w)||_0), \end{aligned} \tag{25}$$

provided by $w, \chi, \gamma(\cdot, w) \in L^\infty(\Omega)$, where $p > 3$, C_a is the maximum of $|\alpha_y|$, $|\alpha_{yy}|$, $|\beta_{yy}|$ and $|g_{yy}|$ on $\bar{\Omega} \times [-a, a]$ and ψ_I is the nodal linear Lagrange interpolant of ψ.

Proof First, by using (18) and (23) with $w = p^i$, $\psi = \phi$, $\chi = p_h^i$, $\kappa = \phi_h$ and $v = v_h$, it is easy to show that p_h^i and ϕ_h are solutions to (20) if and only if (24) holds.

Next, we follow the arguments in [40] to prove (25). Let $\eta(t) = A(w + t(\chi - w), v)$. Since:

$$\eta(1) = \eta(0) + \eta'(0) + \int_0^1 \eta''(t)(1-t)dt,$$

we have:

$$A(\chi, v) = A(w, v) + A'(w, \chi - w, v) + \tilde{R}(w, \chi, v),$$

where $\tilde{R}(w, \chi, v) = \int_0^1 \eta''(t)(1-t)dt$. Compared with (23), it apparently shows that

$$|R(w,\psi,\chi,\kappa,v)| = |B(\chi,\kappa,v) - B(w,\psi,v) + \tilde{R}(w,\chi,v)| \le |B(\chi,\kappa,v) - B(w,\psi,v)| + |\tilde{R}(w,\chi,v)|. \tag{26}$$

For the first term on the right hand side in the above equality, we have:

$$\begin{aligned}|B(\chi,\kappa,v) - B(w,\psi,v)| &= |(\gamma(\cdot,\chi)\nabla\kappa - \gamma(\cdot,w)\nabla\psi, \nabla v)| \\ &\le |(\nabla\kappa(\gamma(\cdot,\chi) - \gamma(\cdot,w)), \nabla v)| + |(\gamma(\cdot,w)(\nabla\kappa - \nabla\psi), \nabla v)| \\ &\le |(\nabla\kappa(\gamma(\cdot,\chi) - \gamma(\cdot,w)), \nabla v)| \\ &+ |(\gamma(\cdot,w)(\nabla\psi - \nabla\psi_I), \nabla v)| + |(\gamma(\cdot,w)(\nabla\psi_I - \nabla\kappa), \nabla v)|. \end{aligned} \tag{27}$$

The estimate of $|(\gamma(\cdot,w)(\nabla\psi - \nabla\psi_I), \nabla v)|$ in (27) is similar to (13). Hence, we can obtian:

$$|(\gamma(\cdot,w)(\nabla\psi - \nabla\psi_I), \nabla v)| \le \sum_\tau (\|\gamma(\cdot,w) - \bar{\gamma}(\cdot,w)\|_{0,\infty,\tau}\|\nabla\psi - \nabla\psi_I\|_{0,\tau}\|\nabla v\|_{0,\tau}) + C((\nabla\psi - \nabla\psi_I), \nabla v).$$

It follows from (7) and (6) that:

$$|(\gamma(\cdot,w)(\nabla\psi - \nabla\psi_I), \nabla v)| \le Ch^2||\nabla v||_0. \tag{28}$$

Inserting (28) into (27), we can have:

$$|B(\chi,\kappa,v) - B(w,\psi,v)| \le C(h^2 + ||\nabla\psi_I - \nabla\kappa||_0 + ||\nabla\kappa||_{0,\infty}||\gamma(\cdot,\chi) - \gamma(\cdot,w)||_0)||\nabla v||_0. \tag{29}$$

On the other hand, according to Lemma 3.1 in [40], $|\tilde{R}(w,\chi,v)|$ can be bounded by:

$$\begin{aligned}|\tilde{R}(w,\chi,v)| \le\ & C_a||v||_1(||w-\chi||_{1,3}||w-\chi||_1 \\ &+ (||\nabla w||_{0,p} + ||\nabla\chi||_{0,p})||w-\chi||_{1,3}||w-\chi||_1). \end{aligned} \tag{30}$$

Inserting (29) and (30) into (26), we complete the proof. □

Corollary 2.1 *If $\gamma(\cdot,u)\in L^{\infty}(\Omega)$, $\forall u\in H_0^1(\Omega)$ and satisfies:*

$$||\gamma(\cdot,u)-\gamma(\cdot,v)||_0\le C||u-v||_0,\quad \forall u,v\in H_0^1(\Omega),$$

then

$$\begin{aligned}|R(w,\psi,\chi,\kappa,v)| \;\le\; & C_a||v||_1(||w-\chi||_{1,3}||w-\chi||_1+(||\nabla w||_{0,p}+||\nabla\chi||_{0,p})||w-\chi||_{1,3}||w-\chi||_1\\ &+\;h^2+||\nabla\psi_I-\nabla\kappa||_0+||\nabla\kappa||_{0,\infty}||\chi-w||_0).\end{aligned}\tag{31}$$

3 Error estimates

In this section, we first present the error estimates in H^1 norm for the PNP equations (3). Comparing with the estimates shown in [42], we improve the results by voiding using the assumption $p_h^i\in L^{\infty}(\Omega)$. Second, we show the H^1 norm error estimates for the nonlinear PNP model (15).

3.1 Error estimates for steady-state Poisson-Nernst-Planck equations

First, we present the error estimates for the electrostatic potential ϕ.

Theorem 3.1 *Let (ϕ,p^i) and (ϕ_h,p_h^i) be solutions to (4) and (5), respectively. If $\phi\in H^2(\Omega)$, then we have:*

$$||\phi-\phi_h||_1\le Ch+\sum_{i=1}^{n}||p^i-p_h^i||_0.\tag{32}$$

Proof It follows from (4) and (5) that:

$$(\sum_{i=1}^{n}q^i(p^i-p_h^i),v_h)=(\nabla(\phi-\phi_h),\nabla v_h)=(\nabla(\phi-\phi_I+\phi_I-\phi_h),\nabla v_h),\quad \forall v_h\in S_0^h.$$

Hence:

$$(\nabla(\phi_I-\phi_h),\nabla v_h)=-(\nabla(\phi-\phi_I),\nabla v_h)+(\sum_{i=1}^{n}q^i(p^i-p_h^i),v_h).$$

Taking $v_h=\phi_I-\phi_h$, from (6) and Poincaré inequality, we obtain:

$$\begin{aligned}||\nabla(\phi_I-\phi_h)||_0^2 &= -(\nabla(\phi-\phi_I),\nabla(\phi_I-\phi_h))+(\sum_{i=1}^{n}q^i(p^i-p_h^i),\phi_I-\phi_h)\\ &\le C(h+\sum_{i=1}^{n}||p^i-p_h^i||_0)||\nabla(\phi_I-\phi_h)||_0.\end{aligned}$$

Thus:

$$||\phi-\phi_h||_1\le||\phi-\phi_I||_1+||\phi_I-\phi_h||_1\le C(h+\sum_{i=1}^{n}||p^i-p_h^i||_0).$$

This completes the proof of the theorem. □

Next, we can present the error estimates for the concentration p^i.

Theorem 3.2 *Let (ϕ, p^i) and (ϕ_h, p_h^i) be the solutions to (4) and (5), respectively. If $\phi \in H^3(\Omega) \cap W^{2,\infty}(\Omega)$, $p^i \in W^{2,\infty}(\Omega)$ and $f \in L^4(\Omega)$ then we have:*

$$||p^i - p_h^i||_1 \leq C \left(h + \sum_{i=1}^{n} ||p^i - p_h^i||_0 \right). \tag{33}$$

Proof From (4) and (5), we have:

$$\begin{aligned}(\nabla(p^i - p_h^i), \nabla v_h) \quad &+(p^i \nabla\phi - p_h^i \nabla\phi_h, \nabla v_h) = (\nabla(p_I^i - p_h^i), \nabla v_h) \\ &+(\nabla(p^i - p_I^i), \nabla v_h) + (p^i \nabla\phi - p_h^i \nabla\phi_h, \nabla v_h) = 0.\end{aligned}$$

Hence:

$$(\nabla(p_I^i - p_h^i), \nabla v_h) = -(\nabla(p^i - p_I^i), \nabla v_h) - (p^i(\nabla\phi - \nabla\phi_h), \nabla v_h) - (\nabla\phi_h(p^i - p_h^i), \nabla v_h).$$

Taking $v_h = p_I^i - p_h^i$ and by using (6), (9) and (32), we have:

$$\begin{aligned}||\nabla(p_I^i - p_h^i)||_0^2 \quad = \quad & -(\nabla(p^i - p_I^i), \nabla(p_I^i - p_h^i)) - (p^i(\nabla\phi - \nabla\phi_h), \nabla(p_I^i - p_h^i)) \\ & -(\nabla\phi_h(p^i - p_h^i), \nabla(p_I^i - p_h^i)). \\ \leq \; & C \left(||\nabla p^i - \nabla p_I^i||_0 + ||p^i||_{0,\infty} ||\nabla\phi - \nabla\phi_h||_0 + ||\nabla\phi_h||_{0,\infty} ||p^i - p_h^i||_0 \right) \\ & \quad ||\nabla(p_I^i - p_h^i)||_0 \\ \leq \; & C \left(h + \sum_{i=1}^{n} ||p^i - p_h^i||_0 \right) ||\nabla(p_I^i - p_h^i)||_0.\end{aligned}$$

Hence:

$$||p^i - p_h^i||_1 \leq ||p^i - p_I^i||_1 + ||p_I^i - p_h^i||_1 \leq C \left(h + \sum_{i=1}^{n} ||p^i - p_h^i||_0 \right).$$

This completes the proof. □

From Theorems 3.1 and 3.2, we can easily get the following corollary.

Corollary 3.1 *Let (ϕ, p^i) and (ϕ_h, p_h^i) be the solutions to (4) and (5), respectively. If the assumptions of Theorem 3.2 hold and $\|p^i - p_h^i\|_0 \leq Ch$, then we have:*

$$\|\phi - \phi_h\|_1 + ||p^i - p_h^i||_1 \leq Ch. \tag{34}$$

The error estimate (34) holds based on the assumption $\|p^i - p_h^i\|_0 \leq Ch$. Up to now, there is no L^2 norm error estimate of p_h^i for the steady-state PNP equations. Recently, we present an optimal L^2 norm error estimate of the finite element approximation p_h^i in [34] for a time-dependent PNP equations, but the arguments used in [34] can not be successfully applied to the steady-state model because of the difference between the steady-state and time-dependent PNP equations. Although there is no theoretical proof for this assumption, many numerical examples including PNP equations for practical biological problems show that the second-order accuracy could be obtained when we apply piecewise linear finite elements on the tetrahedral mesh to discretize the equations (see Tables 1 and 6 in Section 5 and also Figs. 3 and 5 in our work [42], where Fig. 5 shows the results of a pratical biological problem).

3.2 Error estimates for nonlinear Poisson-Nernst-Planck equations

In this subsection, we shall present the error estimates for the nonlinear PNP (15) on the basis of Xu and zhou's work in [40]. First, we need some lemmas for the Galerkin projection.

Lemma 3.1 [40] *Let $P_h' : H_0^1(\Omega) \to S_0^h$ be defined by:*

$$A'(p^i, p^i - P_h' p^i, v_h) = 0, \qquad \forall v_h \in S_0^h. \tag{35}$$

If $p^i \in H_0^2(\Omega)$, then we have:

$$||p^i - P_h' p^i||_{1,t} \lesssim Ch^{3/t-1/2}||p^i||_2, \; t \geq 2, \tag{36}$$

and

$$||P_h' p^i||_{1,p} \leq C||p^i||_2. \tag{37}$$

Lemma 3.2 *Suppose the assumptions of Corollary 2.1 and Lemma 3.1 hold. Let (ϕ, p^i) and (ϕ_h, p_h^i) be solutions to (18)-(19) and (20)-(21), respectively. If $\phi \in H^3(\Omega) \cap W^{2,\infty}(\Omega)$, $f \in L^4(\Omega)$, $||p^i - p_h^i||_0 \leq Ch^2$ and $h << 1$, then we have:*

$$||p_h^i - P_h' p^i||_1 \leq Ch^{\frac{3}{2}}. \tag{38}$$

Proof First, we shall prove:

$$||p_h^i - P_h' p^i||_1 \leq Ch. \tag{39}$$

Let $\Phi : S_0^h \to S_0^h$ be defined by, for $v \in S_0^h$,

$$A'(p^i, \Phi(v), v_h) = A'(p^i, p^i, v_h) - R(p^i, \phi, v, \phi_h, v_h), \qquad \forall v_h \in S_0^h. \tag{40}$$

Obviously, Φ is continuous. Define:

$$B = \{v \in S_0^h : ||v - P_h' p^i||_1 \leq Ch\}.$$

If $\Phi(B) \subset B$, by Brouwer's fixed point theorem, then there exists a fixed point $p_h^i \in B$ and $\Phi(p_h^i) = p_h^i$ holds. By (40) and Lemma 2.7, we obtain that p_h^i is the solution to (20) and (39) holds. Hence, to derive (39), we only need to show $\Phi(B) \subset B$. For any $v \in B$, from (35) and (40), we have:

$$A'(p^i, \Phi(v) - P_h' p^i, v_h) = -R(p^i, \phi, v, \phi_h, v_h). \qquad \forall v_h \in S_0^h.$$

Since $\Phi(v) - P_h' p^i \in S_0^h$, by Lemma 2.6, we have:

$$||\Phi(v) - P_h' p^i||_1 \leq C \sup_{\varphi \in S_0^h} \frac{A'(p^i, \Phi(v) - P_h' p^i, \varphi)}{\|\varphi\|_1} \leq C \sup_{\varphi \in S_0^h} \frac{|R(p^i, \phi, v, \phi_h, \varphi)|}{\|\varphi\|_1}.$$

From (31) and $v \in B$, we get:

$$||\Phi(v) - P_h' p^i||_1 \leq C(||p^i - v||_{1,3}||p^i - v||_1 + h^2 + ||\nabla\phi_I - \nabla\phi_h||_0 + ||\nabla\phi_h||_{0,\infty}||p^i - v||_0).$$

The following estimate can be obtained from (8) and (9):

$$||\Phi(v) - P_h' p^i||_1 \leq C\left(||p^i - v||_{1,3}||p^i - v||_1 + h^2 + \sum_{i=1}^{n}||p^i - p_h^i||_0 + ||p^i - v||_0\right), \quad (41)$$

To estimate the first term in the right hand, first by inverse inequality and $v \in B$, we get:

$$||P_h' p^i - v||_{1,3} \leq Ch^{-\frac{1}{2}}||P_h' p^i - v||_1 \leq Ch^{\frac{1}{2}}. \quad (42)$$

Then according to (36) and (42), we have:

$$||p^i - v||_1||p^i - v||_{1,3} \leq (||p^i - P_h' p^i||_{1,3} + ||P_h' p^i - v||_{1,3})(||p^i - P_h' p^i||_1 + ||P_h' p^i - v||_1) \leq Ch^{\frac{3}{2}}. \quad (43)$$

Inserting (43) into (41), it yields:

$$||\Phi(v) - P_h' p^i||_1 \leq C\left(h^{\frac{3}{2}} + h^2 + \sum_{i=1}^{n}||p^i - p_h^i||_0 + ||p^i - v||_0\right). \quad (44)$$

By using (36) and $v \in B$, we have:

$$||p^i - v||_0 \leq ||p^i - P_h' p^i||_0 + ||P_h' p^i - v||_0 \leq Ch. \quad (45)$$

Inserting (45) into (44) and using the assumption $||p^i - p_h^i||_0 \leq Ch^2$, we have:

$$||\Phi(v) - P_h' p^i||_1 \leq C(h^{\frac{3}{2}} + h^2 + h),$$

Since $h < 1$, we have:

$$||\Phi(v) - P_h' p^i||_1 \leq Ch,$$

which leads to $\Phi(B) \subset B$. By using Brouwer's fixed point theorem, there is a fixed point p_h^i such that $p_h^i = \Phi(p_h^i)$. Hence, p_h^i is the solution to (20) and (39) holds. Furthermore, from (44), there holds:

$$\begin{aligned}||p_h^i - P_h' p^i||_1 &= \|\Phi(p_h^i) - p_h^i p^i\|_1 \\ &\leq C\left(h^{\frac{3}{2}} + h^2 + \sum_{i=1}^{n}||p^i - p_h^i||_0 + ||p^i - p_h^i||_0\right)\end{aligned}$$

Then (38) is derived according to the assumption $||p^i - p_h^i||_0 \leq Ch^2$. We finish the proof of this lemma. □

Now we can show the a priori error estimates for the nonlinear PNP model (15).

Theorem 3.3 *Suppose the assumptions of Corollary 2.1 and Lemma 3.1 hold. Let (ϕ, p^i) and (ϕ_h, p_h^i) be solutions to (18)-(19) and (20)-(21), respectively. If $\phi \in H^3(\Omega) \cap W^{2,\infty}(\Omega)$, $f \in L^4(\Omega)$, $||p^i - p_h^i||_0 \leq h^2$ and $h << 1$, then we have:*

$$\|\phi - \phi_h\|_1 + ||p^i - p_h^i||_1 \leq Ch. \quad (46)$$

Proof First, the proof for the estimates of $\|\phi - \phi_h\|_1$ is the same as that for Theorem 3.1, since the difference between nonlinear PNP equations (15) and PNP equations (3) is the first equation in (15), which is not used in this proof. Second, it follows from (36) and (38) that:

$$\begin{aligned}||p^i - p_h^i||_1 &\leq ||p_h^i - P_h' p^i||_1 + ||p^i - P_h' p^i||_1 \\ &\leq Ch.\end{aligned}$$

We complete the proof of this Theorem. □

Similar as Corollary 3.1, error estimate (46) holds when $||p^i - p_h^i||_0 \leq h^2$, which shall be shown by numerical examples in Section 5.

4 Superconvergence

In this section, we shall present superconvergence analysis for both steady-state PNP equations and nonlinear steady-state PNP equations under the assumption that the mesh T^h is uniform. First, we introduce a gradient recovery type operator $G_h : S_0^h \to S^h \times S^h$ which is defined as follows (cf. [41, 43]):

$$G_h v_h = \sum_{z \in \partial^2 T^h} \Big(\sum_{j=1}^{J_z} \alpha_z^j (\nabla v_h)|_{\tau_z^j}(z) \Big) \varphi_z, \quad \forall v_h \in S_0^h.$$

Here φ_z is the basis function, $\partial^2 T^h$ is the set of vertices of the triangulation T^h and $\bigcup\limits_{j=1}^{J_z} \tau_z^j = \omega_z$, where τ_z^j represents the jth element which includes the vertice $z \in \partial^2 T^h$. The coefficient α_z^j satisfies $\sum\limits_{j=1}^{J_z} \alpha_z^j = 1$ and $\alpha_z^j \geq 0$. For example, $\alpha_z^j = \frac{1}{J_z}$ or $\alpha_z^j = \frac{|\tau_z^j|}{|\omega_z|}$. Here $(\nabla v_h)|_{\tau_z^j}$ is understood in the sense of trace in τ_z^j.

From the definition of the operator G_h and the properties of the basis function, we can easily get the following estimates:

Lemma 4.1 *There holds:*

$$\|G_h w_h\|_0 \leq \|\nabla w_h\|_0, \quad \forall w_h \in S^h, \tag{47}$$

and

$$\|G_h w_h\|_{0,\infty} \leq \|\nabla w_h\|_{0,\infty}, \quad \forall w_h \in S^h. \tag{48}$$

Proof

$$\|G_h w_h\|_0 = \left(\sum_{\tau \in T^h} \int_\tau \Big| \sum_{z \in \partial^2 T^h} \Big(\sum_{j=1}^{J_z} \alpha_z^j (\nabla w_h)|_{\tau_z^j}(z) \Big) \varphi_z \Big|^2 dV \right)^{\frac{1}{2}}.$$

Denote the number of vertice z satisfying $\varphi_z \neq 0$ on the element $\tau \in T^h$ by m_τ. It is known that there exists a constant C_0 independently of h, such that $m_\tau < C_0$. Then we have:

$$\begin{aligned}\|G_h w_h\|_0 &\leq C(\sum_{\tau\in T^h}\int_\tau \left|\nabla w_h\right|^2 dV)^{\frac{1}{2}}\\ &\leq C\|\nabla w_h\|_0,\end{aligned}$$

where we have used the property of basis function $|\varphi_z| \leq 1$ and J_z is bounded. Thus, we get (47). Similarly, for any $x_0 \in \Omega$, we have:

$$\begin{aligned}|G_h w_h(x_0)| &= \Big|\sum_{z\in\partial^2 T^h}\big(\sum_{j=1}^{J_z}\alpha_z^j(\nabla w_h)|_{\tau_z^j}(z)\big)\varphi_z(x_0)\Big|\\ &\leq C\|\nabla w_h\|_{0,\infty}\Big|\sum_{z\in\partial^2 T^h}\varphi_z(x_0)\Big|\\ &\leq C\|\nabla w_h\|_{0,\infty}.\end{aligned}$$

Hence, $\|G_h w_h\|_{0,\infty} \leq C\|\nabla w_h\|_{0,\infty}$. The proof is completed. □

Lemma 4.2 [43] *If $u \in H_0^3(\Omega)$, then:*

$$\|(\nabla u)_I - G_h u_I\|_0 \leq Ch^{\frac{3}{2}}, \tag{49}$$

where u_I is the nodal linear Lagrange interpolant of u.

4.1 Superconvergence for the steady-state Poisson-Nernst-Planck equations

Now, we present the superconvergence results for the steady-state PNP equations (3).

Theorem 4.1 *Let (p^i, ϕ) and (p_h^i, ϕ_h) be the solutions to (4) and (5), respectively. If $\phi \in H_0^3(\Omega)$, then:*

$$\|\nabla\phi - G_h\phi_h\|_0 \leq C(h^{\frac{3}{2}} + \sum_{i=1}^n \|p^i - p_h^i\|_0). \tag{50}$$

Proof It follows from (6), (8), (49), and (47) that:

$$\begin{aligned}\|\nabla\phi - G_h\phi_h\|_0 &\leq \|\nabla\phi - (\nabla\phi)_I\|_0 + \|(\nabla\phi)_I - G_h\phi_I\|_0 + \|G_h\phi_I - G_h\phi_h\|_0\\ &\leq C(h^{\frac{3}{2}} + \sum_{i=1}^n \|p^i - p_h^i\|_0).\end{aligned}$$

This completes the proof. □

Theorem 4.2 *Let (p^i, ϕ) and (p_h^i, ϕ_h) be the solutions to (4) and (5), respectively. If $\phi \in H_0^3(\Omega) \cap W^{2,\infty}(\Omega)$ and $p^i \in H_0^3(\Omega) \cap L^\infty(\Omega)$, then we have the following estimate:*

$$\|\nabla p^i - G_h p_h^i\|_0 \leq C(h^{\frac{3}{2}} + \|p^i - p_h^i\|_0). \tag{51}$$

Proof Similar to the proof of Theorem 4.1, we have:

$$\|\nabla p^i - G_h p_h^i\|_0 \leq \|\nabla p^i - (\nabla p^i)_I\|_0 + \|(\nabla p^i)_I - G_h p_I^i\|_0 + \|G_h p_I^i - G_h p_h^i\|_0, \quad (52)$$

where $(\nabla p^i)_I$ and p_I^i are the nodal linear Lagrange interpolant of ∇p^i and p^i, respectively. By (6), (47), and (49), we get:

$$\|\nabla p^i - G_h p_h^i\|_0 \leq C(h^{\frac{3}{2}} + \|\nabla p_I^i - \nabla p_h^i\|_0). \quad (53)$$

It remains to estimate $\|\nabla p_I^i - \nabla p_h^i\|_0$. Note that for any $v_h \in S_0^h$,

$$(\nabla(p_h^i - p_I^i), \nabla v_h) = (\nabla(p_h^i - p^i), \nabla v_h) + (\nabla(p^i - p_I^i), \nabla v_h). \quad (54)$$

For the first term, subtracting (4) from (5) and note that q^i is a constant, we have:

$$\begin{aligned}(\nabla(p_h^i - p^i), \nabla v_h) &= q^i(p^i\nabla\phi - p_h^i\nabla\phi_h, \nabla v_h)\\ &= (p^i\nabla\phi - p_h^i\nabla\phi_h, \nabla(q^i v_h))\\ &\leq C(h^2 + \|p^i - p_h^i\|_0)\|\nabla v_h\|_0,\end{aligned} \quad (55)$$

where (10) is used in the last inequality. Inserting (55) into (54) and by (7), we get:

$$(\nabla(p_h^i - p_I^i), \nabla v_h) \leq C(h^2 + \|p^i - p_h^i\|_0)\|\nabla v_h\|_0.$$

Taking $v_h = p_h^i - p_I^i$, we obtain:

$$\|\nabla(p_h^i - p_I^i)\|_0 \leq C(h^2 + \|p^i - p_h^i\|_0). \quad (56)$$

Combining (53) and (56), we obtain the desired result. □

Corollary 4.1 *Under the assumptions of Theorem 4.2, if $\|p^i - p_h^i\|_0 \leq Ch^{\frac{3}{2}}$, then we can get:*

$$\|\nabla\phi - G_h\phi_h\|_0 \leq Ch^{\frac{3}{2}}, \quad (57)$$

and

$$\|\nabla p^i - G_h p_h^i\|_0 \leq Ch^{\frac{3}{2}}. \quad (58)$$

4.2 Superconvergence for the nonlinear steady-state Poisson-Nernst-Planck equations

In this subsection, we present the superconvergence result for nonlinear steady-state PNP equations (15). For this sake, first we introduce the following lemma.

Lemma 4.3 *(see, e.g., [3, 10, 46]) If $u \in H_0^3(\Omega)$, then:*

$$||P_h' u - u_I|| \leq Ch^2, \quad (59)$$

where $P_h' : H_0^1(\Omega) \to S_0^h$ is defined by:

$$A'(u; w - P_h' w, v) = 0, \quad \forall v \in S_0^h,$$

and u_I is the standard Lagrange interpolation of u.

Now we can present the superconvergence results for the solution of the nonlinear PNP equations.

Theorem 4.3 *Let* (p^i, ϕ) *and* (p_h^i, ϕ_h) *be the solutions to (18)–(19) and (20)–(21), respectively. If* $\phi \in H_0^3(\Omega) \cap W^{2,\infty}(\Omega)$, $p^i \in H_0^3(\Omega) \cap L^\infty(\Omega)$ *and* $||p^i - p_h^i||_0 \leq Ch^2$, *then we have the following estimate:*

$$\|\nabla \phi - G_h \phi_h\|_0 + \|\nabla p^i - G_h p_h^i\|_0 \leq C h^{\frac{3}{2}}. \tag{60}$$

Proof First, the proof for the estimates of $\|\nabla \phi - G_h \phi_h\|_1$ is the same as that for Theorem 4.1, since the difference between nonlinear PNP equations (15) and PNP equations (3) is the first equation in (15), which is not used in this proof. Second, similar to the proof of Theorem 4.2, we have:

$$\|\nabla p^i - G_h p_h^i\|_0 \leq \|\nabla p^i - (\nabla p^i)_I\|_0 + \|(\nabla p^i)_I - G_h p_I^i\|_0 + \|G_h p_I^i - G_h p_h^i\|_0, \tag{61}$$

where $(\nabla p^i)_I$ and p_I^i are the nodal linear Lagrange interpolant of ∇p^i and p^i, respectively. By (6), (49), and (47), we get:

$$\|\nabla p^i - G_h p_h^i\|_0 \leq C(h^{\frac{3}{2}} + \|\nabla p_I^i - \nabla p_h^i\|_0). \tag{62}$$

It remains to estimate $\|\nabla p_I^i - \nabla p_h^i\|_0$. It follows from (59) and (38) that:

$$\begin{aligned} ||\nabla p_I^i - \nabla p_h^i||_0 &\leq ||p_I^i - P_h' p^i||_1 + ||p_h^i - P_h' p^i||_1 \\ &\leq C h^{\frac{3}{2}} \end{aligned} \tag{63}$$

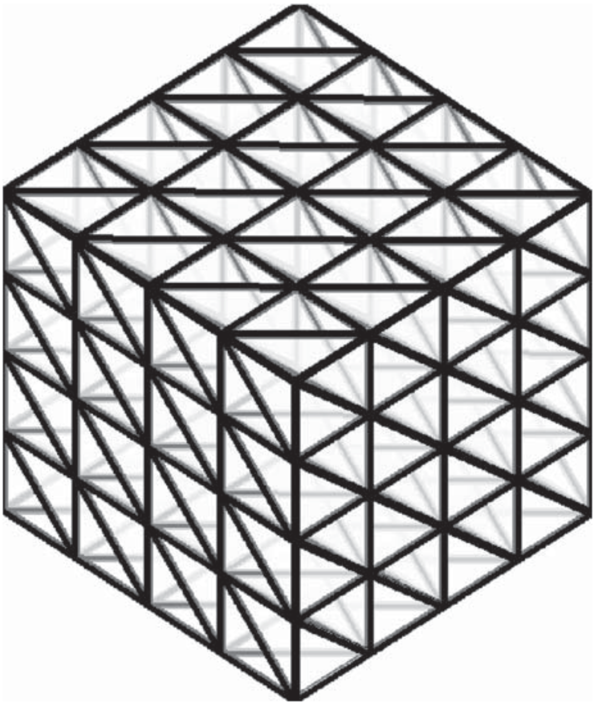

Fig. 1 Tetrahedral mesh division

Combining (62) and (63), we obtain the desired result. □

5 Numerical results

In this section, we report two numerical experiments to illustrate the theoretical results. The first one is a steady-state PNP system and the second one is a nonlinear steady-state PNP system. To implement the numerical experiments, the code is written in CPU-3.20GHz(Intel(R) Core(TM) i5-6500), RAM-8GB, Windows 10 system, Fortran4.0 compiler and all the computations are carried out on the same computer. We use piecewise linear finite elements on a uniform tetrahedral mesh to discretize the equation (see Fig. 1 for the tetrahedral mesh).

Example 5.1 We consider the steady-state PNP equations with an analytic solution as follows:

$$\begin{cases} \nabla\cdot\left(\nabla p^i + q^i p^i \nabla\phi\right) = f_i, \quad \text{in } \Omega, \quad i = 1, 2, \\ -\triangle\phi - \sum_{i=1}^{2} q^i p^i = f_3, \quad \text{in } \Omega. \end{cases} \tag{64}$$

Here the computational domain $\Omega = [0, 1]^3 \subset R^3$ and $q^1 = 1, \quad q^2 = -1$. The boundary condition and the right-hand side functions are chosen such that the exact solution (ϕ, p^1, p^2) is given by:

$$\begin{cases} \phi = x(x-1)y(y-1)z(z-1), \\ p^1 = \sin 2\pi x \sin 2\pi y \sin 2\pi z, \\ p^2 = \sin 3\pi x \sin 3\pi y \sin 3\pi z. \end{cases}$$

The algorithm for getting the finite element solution $(\phi_h, \ p_h^1, \ p_h^2)$ of Example 5.1 is as follows:

Algorithm 1 (FEM with Gummel iteration for PNP).

Step 1. Given initial vaule $p_h^{i,0} \in S_0^h, \ i = 1, 2$ and tolerance $\delta = 10^{-5}$.
Step 2. For $m \geq 0$, find $\phi_h^{m+1} \in S_0^h$ such that

$$\left(\nabla\phi_h^{m+1}, \nabla w_h\right) = \left(f_3 + \sum_{i=1}^{2} q^i p_h^{i,m}, w_h\right), \forall w_h \in S_0^h.$$

Step 3. Find $p_h^{i,m+1} \in S_0^h$ such that

$$(\nabla p_h^{i,m+1}, \nabla w_h) + (q^i p_h^{i,m+1} \nabla\phi_h^{m+1}, \nabla w_h) = (f_i, w_h), \quad i = 1, 2, \forall w_h \in S_0^h.$$

Step 4. If $\|p_h^{1,m+1} - p_h^{1,m}\| + \|p_h^{2,m+1} - p_h^{2,m}\| \leq \delta$, then stop. Otherwise, let $m := m + 1$ and go to step 2.

Table 1 The L^2 error between the exact solutions and the finite element solutions for Example 5.1

h	$\|p_h^1 - p^1\|_0$	Order	$\|p_h^2 - p^2\|_0$	Order
1/4	2.43E−01	–	3.25E−01	–
1/8	9.13E−02	1.41E+00	1.71E−01	0.93E+00
1/16	2.58E−02	1.82E+00	5.56E−02	1.62E+00
1/32	6.65E−03	1.95E+00	1.49E−02	1.89E+00
1/64	1.65E−03	2.01E+00	3.82E−03	1.96E+00

The order represents the convergence order in L^2 norm

Table 2 The H^1 error between the exact solutions and the finite element solutions for Example 5.1

h	$\|p^1 - p_h^1\|_1$	Order	$\|p^2 - p_h^2\|_1$	Order	$\|\phi_h - \phi\|_1$	Order
1/4	3.03E+00	–	5.39E+00	–	2.05E−02	–
1/8	1.81E+00	0.73E+00	3.74E+00	0.52E+00	1.27E−02	0.69E+00
1/16	9.57E−01	0.92E+00	2.10E+00	0.83E+00	5.55E−03	1.19E+00
1/32	4.85E−01	0.97E+00	1.06E+00	0.95E+00	2.38E−03	1.22E+00
1/64	2.44E−01	0.99E+00	5.47E−01	0.98E+00	1.11E−03	1.09E+00

The order represents the convergence order in H^1 norm

Table 3 The errors of $G_h\phi_h$ and $\nabla\phi_h$ for Example 5.1

h	$\|\nabla\phi - G_h\phi_h\|_0$	Order	$\|\nabla\phi - \nabla\phi_h\|_0$	Order
1/4	1.44E−02	–	2.05E−02	–
1/8	7.66E−03	0.91E+00	1.27E−02	0.69E+00
1/16	3.36E−03	1.18E+00	5.54E−03	1.18E+00
1/32	1.12E−03	1.59E+00	2.38E−03	1.22E+00
1/64	3.28E−04	1.76E+00	1.11E−03	1.09E+00

Table 4 The errors of $G_h p_h^1$ and ∇p_h^1 for Example 5.1

h	$\|\nabla p^1 - G_h p_h^1\|_0$	Order	$\|\nabla p^1 - \nabla p_h^1\|_0$	Order
1/4	3.19E+00	–	3.02E+00	–
1/8	1.65E+00	0.95E+00	1.81E+00	0.75E+00
1/16	5.88E−01	1.48E+00	9.57E−01	0.92E+00
1/32	1.77E−01	1.72E+00	4.85E−01	0.97E+00
1/64	5.23E−02	1.76E+00	2.44E−01	0.99E+00

First, Table 1 shows that the convergence orders in L^2 norm for both positive ion concentration p_h^1 and negative ion concentration p_h^2 are second order, which satisfies the assumption condition $\|p^i - p_h^i\|_0 \le Ch^2, i = 1, 2$ shown in Corollary 3.1. Table 2 shows that the errors in H^1 norm are first order, which coincides with the theoretical results in Corollary 3.1. Second, from Tables 3, 4, and 5, we see that the convergence orders of the superconvergence errors for both $G_h\phi_h$ and $G_h p_h^i$ approximate 1.8, which is better than the theoretical results shown in Corollary 4.1; the reason of which needs further investigation. Moreover, the errors for $G_h\phi_h$ and $G_h p_h^i$ are compared with the errors for $\nabla\phi_h$ and ∇p_h^i respectively, which indicates the accuracy of the gradient of finite element approximation could be improved for the PNP equations by using the gradient recovery operator G_h .

Example 5.2 Consider the following nonlinear steady-state PNP equations:

$$\nabla \cdot \Big(\nabla p^i + q^i p^i \nabla\phi + p^i \nabla sech^2(p^i)\Big) = f_i, \text{ in } \Omega, \quad i = 1, 2, \tag{65}$$

$$-\triangle\phi - \sum_{i=1}^{2} q^i p^i = f_3, \text{ in } \Omega. \tag{66}$$

Here the computational domain $\Omega = [0, 1]^3 \subset R^3$ and $q^1 = 1, \quad q^2 = -1$. The boundary condition and the right-hand side functions are chosen such that the exact solution (ϕ, p^1, p^2) is given by:

$$\begin{cases} \phi = \sin\pi x \, \sin\pi y \, \sin\pi z, \\ p^1 = \sin 2\pi x \, \sin 2\pi y \, \sin 2\pi z, \\ p^2 = \sin 3\pi x \, \sin 3\pi y \, \sin 3\pi z. \end{cases} \tag{67}$$

This model is a simplified modified PNP model from [23] and the corresponding practical ion channel model is studied in Example 6.3. Comparing (65) with (15), we see that $\alpha(x, p^i) = 1 - 2sech^2(p^i)tanh(p^i)p^i$, $\beta(x, p^i) = 0$, $\gamma(x, p^i) = q^i p^i$, $g(x, p^i) = f_i$. Obviously, when $p^i \in R$, we have $\alpha(x, p^i) > 0$. From (67), since the concentration $p^i \in [0, 1]$, we have $sech^2(p^i)tanh(p^i) < 1/2$ and $\alpha(x, p^i) > 0$. Hence, the assumption (17) is satisfied, which indicates that $L'(p)$ is isomorphic. According to Lax-Milgram Theorem, it follows that the solution (ϕ, p^i) is unique. Second, since $\gamma(x, p^i) = q^i p^i$ and the solution shown by (67) satisfies the assumptions of Corollary 2.1 and Lemma 2.7 respectively, from Theorem 3.3, we know that

Table 5 The errors of $G_h p_h^2$ and ∇p_h^2 for Example 5.1

h	$\|\nabla p^2 - G_h p_h^2\|_0$	Order	$\|\nabla p^2 - \nabla p_h^2\|_0$	Order
1/4	5.65E+00	–	5.38E−00	–
1/8	3.89E+00	0.59E+00	3.74E−00	0.52E+00
1/16	1.68E+00	1.21E+00	2.10E−00	0.83E+00
1/32	5.29E−01	1.66E+00	1.09E−00	0.95E+00
1/64	1.51E−01	1.80E+00	5.47E−01	0.98E+00

if $\|p^i - p_h^i\|_0 \leq Ch$, then the error estimates in H^1 norms are first order for this nonlinear PNP equation.

The following Algorithm 2 is used to obtain the finite element solution $(\phi_h,\ p_h^1,\ p_h^2)$ of Example 5.2.

Algorithm 2 (FEM with Gummel iteration for nonlinear PNP).

Step 1. Given initial vaule $p_h^{i,0} \in S_0^h,\ i = 1, 2$ and tolerance $\delta = 10^{-5}$.
Step 2. For $m \geq 0$, find $\phi_h^{m+1} \in S_0^h$ such that

$$\left(\nabla\phi_h^{m+1}, \nabla w_h\right) = \left(f_3 + \sum_{i=1}^{2} q^i p_h^{i,m}, w_h\right), \forall w_h \in S_0^h.$$

Step 3. Find $p_h^{i,m+1} \in S_0^h$ such that

$$(\nabla p_h^{i,m+1}, \nabla w_h) + (q^i p_h^{i,m+1}\nabla\phi_h^{m+1} + p_h^{i,m+1}\nabla sech p_h^{i,m+1}, \nabla w_h) = (f_i, w_h),\quad i = 1, 2, \forall w_h \in S_0^h.$$

Step 4. If $\|p_h^{1,m+1} - p_h^{1,m}\| + \|p_h^{2,m+1} - p_h^{2,m}\| \leq \delta$, then stop. Otherwise, let $m := m + 1$ and go to step 2.

Similar as the results in Example 5.1, Tables 6 and 7 show the errors in L^2 norm and H^1 norm are second order and first order respectively, which verifies the theoretical results in Theorem 3.3. From Tables 8, 9, and 10, the convergence order of the errors for $G_h\phi_h$ and $G_h p_h^i$, i = 1,2 in L^2 norm is more than 1.5, which coincides with the theoretical results in Theorem 4.3 and indicates the gradient recovery operator G_h can improve the accuracy of the gradient of the finite element approximation for this nonlinear PNP model.

6 Application to ion channel problem

In this section, we shall apply the gradient recovery technique to the PNP equations describing a practical ion channel. The PNP equations for ion channel are a complex coupled system, the whole computational efficiency of which is mainly affected by

Table 6 The L^2 norm error between the exact solutions and the finite element solutions

h	$\|p_h^1 - p^1\|_0$	Order	$\|p_h^2 - p^2\|_0$	Order
1/4	2.62E−01	–	3.38E−01	–
1/8	1.16E−01	1.17E+00	2.04E−01	0.72E+00
1/16	3.75E−02	1.63E+00	7.95E−02	1.36E+00
1/32	1.01E−02	1.89E+00	2.36E−02	1.75E+00
1/64	2.62E−03	1.95E+00	6.25E−03	1.91E+00

The order represents the convergence order in L^2 norm for Example 5.2

Table 7 The H^1 error norm between the exact solutions and the finite element solutions

h	$\|\phi - \phi_h\|_1$	Order	$\|p^1 - p_h^1\|_1$	Order	$\|p^2 - p_h^2\|_1$	Order
1/4	9.14E−01	–	3.13E−00	–	5.55E−00	–
1/8	4.80E−01	0.93	1.89E−00	0.73	3.96E−00	0.49
1/16	2.43E−01	0.98	0.98E−00	0.95	2.21E−00	0.84
1/32	1.22E−01	1.00	0.49E−00	1.00	1.11E−00	0.99
1/64	6.09E−02	1.00	0.24E−00	1.00	5.51E−01	1.01

The order represents the convergence order in H^1 norm for Example 5.2

the efficiency of the external iteration. The idea of applying the gradient recovery technique to ion channel problem is similar as that for Examples 5.1 and 5.2. Based on the superconvergence properties, the gradient recovery technique is used as a post-process to improve the accuracy of the gradient approximation. But unlike Examples 5.1 and 5.2, the gradient recovery technique applied in this section is used not only for the post-processing of the final solution but also for the iterative solution in each step of the external iteration, which accelerates the iteration process. Since there is no analytic solution to PNP equations for the ion channel, the numerical solution is further used to compute the current and then compared with the experimental result, which is also different from Examples 5.1 and 5.2.

Next, we shall introduce a nonlinear PNP model for the ion channel and present the corresponding finite element discretization. Then we shall combine the finite element method with the gradient recovery technique to get a new algorithm. After that, we shall present a numerical example, which shows that the new algorithm can improve the efficiency of the external iteration and save much more CPU time for the Gramicidin A ion channel problem.

6.1 Mathematical model

We consider the following nonlinear PNP model for simulating the ion channel with n ion species (cf. [23]),

$$\begin{cases} \nabla \cdot D^i \left(\nabla p^i + \frac{e}{K_B T} q^i p^i \nabla \phi + \frac{e}{K_B T} p^i \nabla \psi \right) = 0, \ \text{ in } \Omega_s, \ 1 \le i \le n, \\ -\nabla \cdot (\epsilon \nabla \phi) - \lambda \sum\limits_{i=1}^{n} q^i p^i = \rho^f, \ \text{ in } \Omega = \Omega_s \cup \Omega_m \subset R^3, \end{cases} \tag{68}$$

Table 8 The errors of $G_h\phi_h$ and $\nabla\phi_h$ for Example 5.2

h	$\|\nabla\phi - G_h\phi_h\|_0$	Order	$\|\nabla\phi - \nabla\phi_h\|_0$	Order
1/4	7.92E−01	–	9.01E−01	–
1/8	3.02E−01	1.39	4.79E−01	0.93
1/16	9,85E−02	1.62	2.43E−01	0.98
1/32	3.13E−02	1.65	1.22E−01	1.00
1/64	1.02E−02	1.62	6.09E−02	1.00

Table 9 The errors of $G_h p_h^1$ and ∇p_h^1 for Example 5.2

h	$\|\nabla p^1 - \nabla G_h p_h^1\|_0$	Order	$\|\nabla p^1 - \nabla p_h^1\|_0$	Order
1/4	3.32E−00	–	3.12E−00	–
1/8	1.86E−00	0.83	1.88E−00	0.73
1/16	6.92E−01	1.43	9.79E−01	0.94
1/32	2.08E−01	1.74	4.89E−01	1.00
1/64	5.98E−02	1.80	2.44E−01	1.00

where

$$\psi = \frac{A}{2}(1-\chi(x)^2)^2 sech^2(\frac{m(x,p^i)-M(x)}{\eta_0})(\frac{4a_i^3\pi M(x)}{3\eta_0}). \tag{69}$$

Here Ω_m represents the membrane and protein region, Ω_s represents the bulk region which includes the channel region, $p^1(x)$ and $p^2(x)$ are the concentrations of the positive ions (Cs^+) and the negative ions (Cl^-) in the bulk solvent respectively, $\phi(x)$ is the electrostatic potential, $D^1(x)$ and $D^2(x)$ are the diffusion coefficients of the positive ions (Cs^+) and the negative ions (Cl^-) respectively, $\varepsilon(x) = \begin{cases} \varepsilon_m, & x \in \Omega_m, \\ \varepsilon_s, & x \in \Omega_s. \end{cases}$ is the dielectric coefficient, $\lambda = \begin{cases} 0, & in\ \Omega_m, \\ 1, & in\ \Omega_s, \end{cases}$ e is the charge for one electron, $K_B T$ is the Boltzmann constant, and $\rho^f(x) = \sum_j q_j \delta(x - x_j)$ is an ensemble of singular atomic charges q_j located at x_j inside the protein. The diffusive interface function (phase function) χ is defined as $\chi = 1/2(tanh(d(x)/\sqrt{2}\eta) + 1)$, where $d(x)$ is the distance function from the antechamber and η is related to the thickness (length) of the antechamber, $M(x) = sR_{ch}^2(x)\pi$ and $m(x, p^i) = \sum_{i=1}^N \frac{4a_i^3\pi}{3} M(x)p^i(x), i = 1, 2$ are the local maximum volume of channel with unit length and the total volume of ions at position x with the unit length, where $R_{ch}^2(x)$ is the channel radius at position x, s is the unit length, and a_i is the radii of the ith ion species, A and η_0 can be viewed as an overall stiffness coefficient and the local stiffness coefficient, respectively.

Table 10 The errors of $G_h p_h^2$ and ∇p_h^2 for Example 5.2

h	$\|\nabla p^2 - \nabla G_h p_h^2\|_0$	Order	$\|\nabla p^2 - \nabla p_h^2\|_0$	Order
1/4	5.70E−00	–	5.54E−00	–
1/8	4.28E−00	0.41	3.95E−00	0.49
1/16	1.99E−00	1.10	2.21E−00	0.84
1/32	6.53E−01	1.61	1.11E−00	0.99
1/64	1.85E−01	1.82	5.51E−01	1.01

System (68) is called the modified PNP channel system in [23]. It takes into account excluded volume effects of particles as well as electric and geometric configurations of the channel (shown by the function ψ in (69)) compared with the classic PNP system.

System (68) is a model with multi-singularities. The source term $\rho^f(x) = \sum_j q_j \delta(x - x_j)$ is a combination of Dirac Delta functions, where j represents the number of the atoms which is usually more than hundreds. To deal with the singularities, the solution to the Poisson equation can be decomposed into $\phi = \phi_s + \phi_m + \phi_r$ to avoid computing the singular equation during the numerical computation (cf. [28]). Define:

$$\phi_s = \frac{1}{4\pi\epsilon_m} \sum_j \frac{q_j}{|x - x_j|},$$

and ϕ_m to be the solution of a Laplace equation:

$$\begin{cases} -\triangle\phi_m = 0, & \Omega_m, \\ \phi_m = -\phi_s, & on \;\; \partial\Omega_m. \end{cases}$$

Then from the second equation in (68), the function ϕ_r satisfies and:

$$-\nabla \cdot (\epsilon \nabla \phi_r) - \lambda \sum_{i=1}^{2} q^i p^i = 0, \;\; \text{in} \;\; \Omega$$

with interface condition:

$$[\epsilon \phi_r] = -(\epsilon_m \nabla(\phi_m + \phi_s)) \cdot \nu, \;\; on \;\; \Gamma,$$

where $\Gamma = \partial\Omega_s \cap \partial\Omega_m$ and ν is the unit normal vector. Note that there is no decomposition of the potential in the solvent region, thus $\phi(x) = \phi_r(x)$ in Ω_s. Hence, the final system for computation after the decomposition becomes:

$$\begin{cases} \nabla \cdot D^i \left(\nabla p^i + \frac{e}{K_B T} q^i p^i \nabla \phi_r + \frac{e}{K_B T} p^i \nabla \psi \right) = 0, \;\; \text{in} \;\; \Omega_s, \;\; 1 \le i \le n, \\ -\nabla \cdot (\epsilon \nabla \phi_r) - \lambda \sum_{i=1}^{2} q^i p^i = 0, \;\; \text{in} \;\; \Omega. \end{cases} \tag{70}$$

To simplify the presentation, in the following we still use ϕ to denote the potential ϕ_r , but keep in mind that the singular and harmonic components are to be added to get the full potential inside molecules.

6.2 Numerical algorithm

We use the finite element method to discretize PNP equations (70). First, we introduce the weak formulation of (70). For simplicity, suppose the solution to (70) satisfies the following boundary condition:

$$\begin{aligned} \phi &= V_{\text{applied}}, \;\; on \;\; \partial\Omega, \\ p^i &= p_\infty, \;\; on \;\; \partial\Omega_s \setminus \Gamma. \end{aligned}$$

where V_{applied} is the applied potential and p_∞ is the given ion concentration. Define:

$$V_\phi = \{v|v \in H^1(\Omega),\ v|_{\partial\Omega} = V_{\text{applied}}\},\quad V_p = \{v|v \in H^1(\Omega_s),\ v|_{\partial\Omega_s\setminus\Gamma} = p_\infty\},$$

The weak formulation is as follows: find solutions $\phi \in V_\phi$, $p^i \in V_p$ satisfying:

$$(D^i\nabla p^i, \nabla v) + (\frac{D^i e}{K_B T} q^i p^i \nabla\phi + \frac{D^i e}{K_B T} p^i \nabla\psi, \nabla v) = 0,\quad \forall v \in H_0^1(\Omega_s),$$

$$(\epsilon\nabla\phi, \nabla w) - (\sum_{i=1}^{2} q^i p^i, w) = 0,\quad \forall w \in H_0^1(\Omega).$$

Suppose $T^h(\Omega)$ is a mesh of size h on domain Ω. Define the following linear finite element space:

$$\begin{aligned}
V_h &= \{v_h|v_h \in H^1(\Omega), v_h|_e \in P^1(e), \forall e \in T^h(\Omega),\ v_h|_{\partial\Omega} = V_{\text{applied}}\},\\
&\quad V_h^0 = \{v_h|v_h \in H^1(\Omega), v_h|_e \in P^1(e), \forall e \in T^h(\Omega),\ v_h|_{\partial\Omega} = 0\},\\
S_h &= \{v_h|v_h \in H^1(\Omega_s), v_h|_e \in P^1(e), \forall e \in T^h(\Omega_s),\ v_h|_{\partial\Omega_s\setminus\Gamma} = p_\infty\}\\
&\quad S_h^0 = \{v_h|v_h \in H^1(\Omega_s), v_h|_e \in P^1(e), \forall e \in T^h(\Omega_s),\ v_h|_{\partial\Omega} = 0\}.
\end{aligned}$$

The finite element approximations to weak solutions are that: finding $\phi_h \in V_h$ and $p_h^i \in S_h$ such that:

$$(D^i\nabla p_h^i, \nabla v_h) + (\frac{D^i e}{K_B T} q^i p_h^i \nabla\phi_h + \frac{D^i e}{K_B T} p_h^i \nabla\psi_h, \nabla v_h) = 0,\quad \forall v_h \in S_h^0, \tag{71}$$

$$(\epsilon\nabla\phi_h, \nabla w_h) - (\sum_{i=1}^{2} q^i p_h^i, w_h) = 0,\quad \forall w_h \in V_h^0, \tag{72}$$

where:

$$\psi_h = \frac{A}{2}(1 - \chi(x)^2)^2 sech^2(\frac{m(x, p_h^i) - M(x)}{\eta_0})(\frac{4a_i^3\pi M(x)}{3\eta_0}).$$

Since system (71)–(72) are a coupled system and defined in different domain, it is more convenient to solve it by a decoupling method such as Gummel iteration [18], which is commonly used in the computation of PNP equations (see, e.g., [24, 28]). The Gummel iteration for (71)–(72) are as follows.

Algorithm 3 FEM with Gummel iteration.

Given initial vaule $p_h^{i,0}$, $i = 1, 2$ and tolerance ϵ.
Step 1. For $k \geq 0$, find ϕ_h^{k+1} such that

$$\left(\varepsilon \nabla \phi_h^{k+1}, \nabla w_h\right) = \left(\lambda \sum_{i=1}^{2} q^i p_h^{i,k}, w_h\right), \forall w_h \in S_0^h. \tag{73}$$

Step 2.

$$(D^i \nabla p_h^{i,k+1}, \nabla v_h) + (\frac{D^i e}{K_B T} q^i p_h^{i,k+1} \nabla \phi_h^{k+1} + \frac{D^i e}{K_B T} p_h^{i,k+1} \nabla \psi_h^{k+1}, \nabla v_h) = 0, \quad i = 1, 2,$$

where

$$\psi_h^{k+1} = \frac{A}{2}(1 - \chi(x)^2)^2 sech^2(\frac{m(x, p_h^{i,k+1}) - M(x)}{\eta_0})(\frac{4a_i^3 \pi M(x)}{3\eta_0}),$$

Step 3. If $\|p_h^{i,k+1} - p_h^{i,k}\|_0 + \|\phi_h^{k+1} - \phi_h^k\|_0 \leq \epsilon$, then exit. Otherwise, let $k := k + 1$ and go to Step 1.

If we use the gradient recovery operator in each step of the above iteration, then we get the following new algorithm.

Algorithm 4 GRFEM with Gummel iteration.

Given initial vaule $p_h^{i,0}$, $i = 1, 2$ and tolerance ϵ.
Step 1. For $k \geq 0$, find ϕ_h^{k+1} such that

$$\left(\varepsilon \nabla \phi_h^{k+1}, \nabla w_h\right) = \left(\lambda \sum_{i=1}^{2} q^i p_h^{i,k}, w_h\right), \forall v_h \in S_0^h, \tag{74}$$

Step 2.

$$(D^i \nabla p_h^{i,k+1}, \nabla v_h) + (\frac{D^i e}{K_B T} q^i p_h^{i,k+1} G_h \phi_h^{k+1} + \frac{D^i e}{K_B T} p_h^{i,k+1} G_h \psi_h^{k+1}, \nabla v_h) = 0, \quad i = 1, 2,$$

where

$$\psi_h^{k+1} = \frac{A}{2}(1 - \chi(x)^2)^2 sech^2(\frac{m(x, p_h^{i,k+1}) - M(x)}{\eta_0})(\frac{4a_i^3 \pi M(x)}{3\eta_0}),$$

Step 3. If $\|p_h^{i,k+1} - p_h^{i,k}\|_0 + \|\phi_h^{k+1} - \phi_h^k\|_0 \leq \epsilon$, then exit. Otherwise, let $k := k + 1$ and go to Step 1.

We see that the difference between Algorithm 3 and Algorithm 4 is that the gradient $\nabla(\phi_h^{k+1} + \psi_h^{k+1})$ is replaced by the term $G_h(\phi_h^{k+1} + \psi_h^{k+1})$, where G_h is the gradient recovery operator defined in Section 4. The number k in Algorithm 1 or Algorithm 2 is called the number of the external iteration in this paper.

6.3 Numerical example

Example 6.3 We consider the modified PNP model for simulating the Gramicidin A ion channel with two ion species in 1 : 1 CsCl solution with valence +1 and −1, respectively:

$$\begin{cases} \nabla \cdot D^i \left(\nabla p^i + \frac{e}{K_BT} q^i p^i \nabla\phi + \frac{e}{K_BT} p^i \nabla\psi\right) = 0, \ \text{in} \ \Omega_s, \ 1 \le i \le 2, \\ -\nabla \cdot (\epsilon\nabla\phi) - \lambda\sum\limits_{i=1}^{2} q^i p^i = \rho^f, \ \text{in} \ \Omega = \Omega_s \cup \Omega_m \subset R^3, \end{cases} \tag{75}$$

where:

$$\psi = \frac{A}{2}(1 - \chi(x)^2)^2 sech^2(\frac{m(x, p^i) - M(x)}{\eta_0})(\frac{4a_i^3\pi M(x)}{3\eta_0}). \tag{76}$$

Here $p^1(x)$ and $p^2(x)$ are the concentrations of the positive ions (Cs^+) and the negative ions (Cl^-) in the bulk solvent respectively, and $\phi(x)$ is the electrostatic potential and the dielectric coefficient $\varepsilon(x) = \begin{cases} 2\varepsilon_0, & x \in \Omega_m, \\ 80\varepsilon_0, & x \in \Omega_s. \end{cases}$

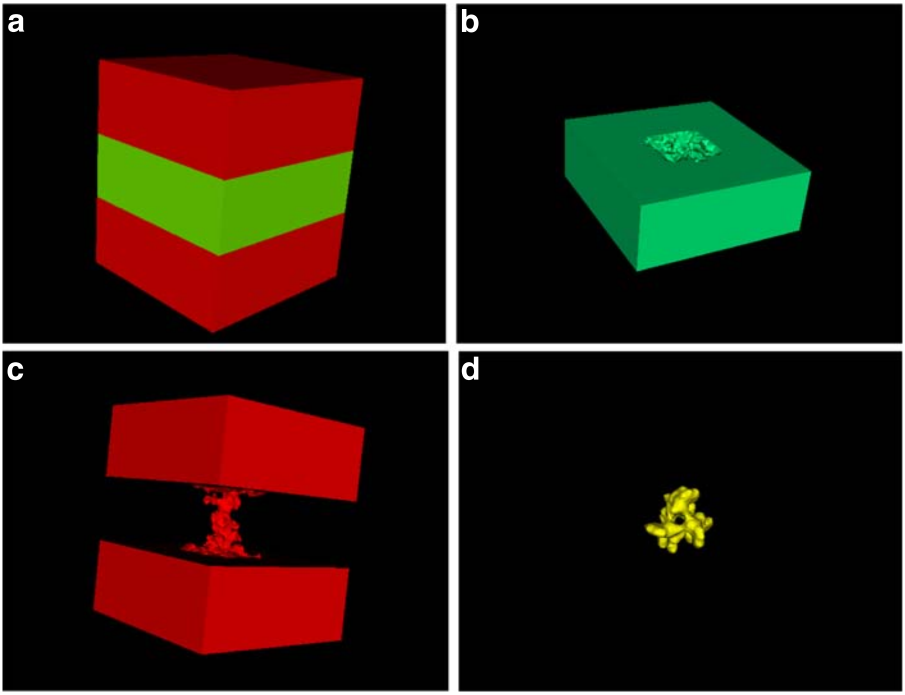

Fig. 2 Membrane and bulk region for Example 6.3. **a** The whole system $\Omega = \Omega_m \cup \Omega_s$, where Ω_m represents the Membrane and protein region and Ω_s represents the bulk region. **b** Membrane and protein region Ω_m. **c** The bulk region Ω_s including the ion channel region. **d** The channel region

Table 11 The parameters for Example 6.3

Variables	Values	Variables	Values
Diffusion coefficient: D^1	$2.0561 \times 10^{-9} m^2/s$	Permittivity of vacuum: ε_0	$8.85 \times 10^{-12} C^2/(N\ m^2)$
Diffusion coefficient: D^2	$2.0321 \times 10^{-9} m^2/s$	Elementary charge: e	$1.6 \times 10^{-19} C$
Boltzmann energy: $K_B T$	$4.14 \times 10^{-21} J$	raii of Cs ion: a_1	$1.81\ \AA$
raii of Cl ion: a_2	$1.67\ \AA$		

Next, we first introduce the region and boundary settings of the solution, and then describe the selection of the parameters. After that, we show the numerical experiment results. The whole computational domain is a box and the membrane part in the macromolecule Ω_m is represented as a slab (see Fig. 2).

Suppose $\Gamma = \partial\Omega_s \cap \partial\Omega_m$ is the internal interface, $\partial\Omega_1$ is the part of boundary of Ω perpendicular to z axis, $\partial\Omega_2$ is the part of boundary of Ω that is along z axis and $\partial\Omega_3 = \partial\Omega_s \setminus \Gamma$. The interface conditions and boundary conditions are described:

$$[\epsilon \nabla \phi] = 0, \quad on \quad \Gamma,$$

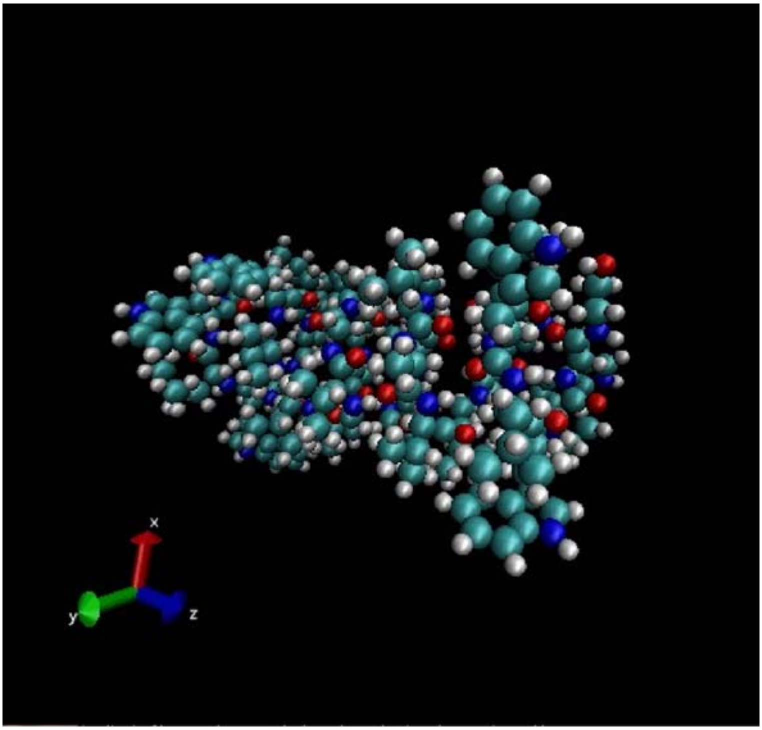

Fig. 3 Atom in the protein of GA ion channel. Totally 553 atoms for this GA ion channel problem

and

$$\begin{cases} \phi = V_{\text{applied}}, & on\ \partial\Omega_1, \\ \frac{\partial \phi}{\partial v} = 0, & on\ \partial\Omega_2, \\ D^i \left(\nabla p^i + \frac{e}{K_B T} q^i p^i \nabla \phi + \frac{e}{K_B T} p^i \nabla \psi \right) \cdot v = 0, & on\ \Gamma, \\ p^i = p_\infty, & on\ \partial\Omega_3, \end{cases} \tag{77}$$

respectively. Here V_{applied} is the applied potential, ν is the unit normal vector, and p_∞ is the given concentration.

This example uses the similar setup as the model presented in [23] and [28]. Some of the main parameters mentioned above are reported in Table 11.

In the simulations, the box $\Omega = [x, y, z] = [-15, 15] \times [-15, 15] \times [-30, 30]\mathring{A}$. In solvent region Ω_s, the gramicidin A channel region is from -16 to 16 $\mathring{A}$ along the z direction. The membrane region is from -19 to 19 $\mathring{A}$ along the z direction. The triangular surface mesh and tetrahedral volume mesh are generated by using TMSmesh [13]. The TMSmesh is a robust tool for meshing molecular Gaussian surfaces and has been shown to be capable of handling molecules consisting of more than one million atoms. The number of the atoms j, the partial charges q_j, and the positions of the atoms x_j in the protein are obtained from protein data bank (see Fig. 3 for the 3D figure of the atoms in the protein), which provides data for the source term $\rho^f = \sum_j q_j \delta(x - x_j)$ in (75).

Totally 224650 triangle elements and 37343 nodes are used in all our computation (see Fig. 4). All the results are computed under Matlab R2012a system. The program is also based on the iFEM toolbox (https://bitbucket.org/ifem/ifem).

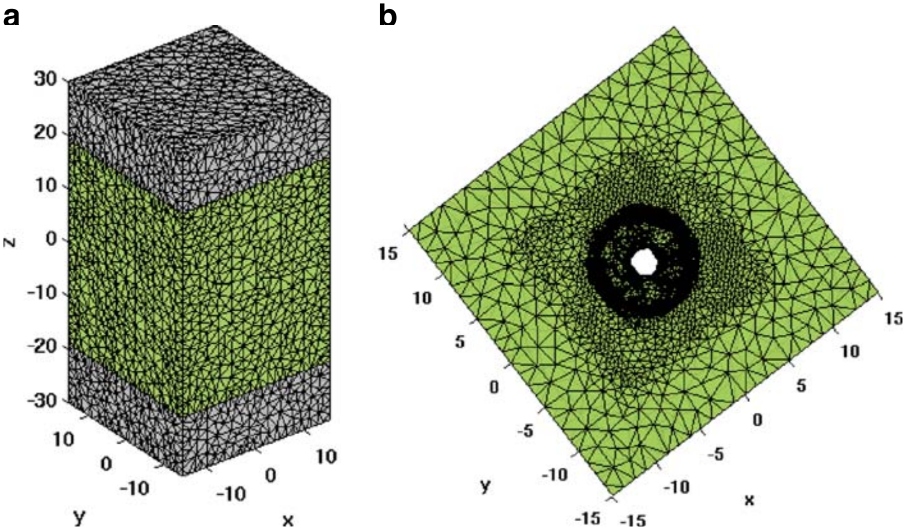

Fig. 4 Mesh for Example 6.3. **a** A 3D mesh for the computational domain illustrates the bulk region, membrane, and protein region. The bulk region is shown in grey. The membrane and protein region are shown in green. The computation domain $\Omega = \Omega_s \cup \Omega_m$ (**b**) A top view of the triangular surface mesh of ion channel with the membrane which is shown as a slab

Since PNP (75) is a complex nonlinear problem, it is difficult to find the analytic solution. To observe the accuracy of Algorithms 3 and 4, the simulation results are compared with the experimental data via the current. Discussion of current is essential in many studies of ion channel problems(see, e.g., [29, 37]). The current is defined by:

$$I = e\int_{\Omega_I} (J_1 - J_2)dS,$$

where Ω_I is any cross section of the channel and J_1 and J_2 given by:

$$J_i = -\nabla \cdot D_i(\nabla p^i + \frac{e}{K_B T} q^i p^i \nabla\phi), i = 1, 2,$$

which are the flux of positive ions and negative ions, respectively.

To get the current, the PNP equations (75) are computed from a variety of voltages, for example, voltage 50 mV, 200 mV, and 400 mV etc. The experimental current data are obtained from Andersen [2] which are used as the reference data for comparison. Table 12 shows the absolute error of the current between the simulation results and experimental data at CsCl concentration 0.02 M and different voltages (mV), which indicates both Algorithms 3 and 4 are efficient for PNP equations (75) (The errors of Algorithms 3 and 4 are acceptable for the practical ion channel problem, cf. Table 1 in [37]). It is also observed from Table 12 that the errors between the currents calculated by Algorithm 4 and the experimental results are a litter bit greater than that by Algorithm 3 under low voltages ($<$ 200 mV). The reason may be that the parameters used in Algorithm 4 are "favorable" to Algorithm 3. The details are as follows. For the practical problems of ion channels, some parameters of the PNP

Table 12 The absolute error of current between the simulation results and experimental data at CsCl concentration 0.02 M and different voltage (mV)

Voltage (mV)	Experimental data (pA)	Algorithm 3 results (pA)	Algorithm 3 error	Algorithm 4 results (pA)	Algorithm 4 error
25	0.13	0.09	0.04	0.04	0.09
50	0.24	0.14	0.10	0.08	0.16
75	0.34	0.16	0.18	0.11	0.23
100	0.40	0.19	0.21	0.15	0.25
150	0.47	0.23	0.24	0.22	0.25
200	0.53	0.27	0.25	0.28	0.25
250	0.56	0.32	0.24	0.35	0.21
300	0.60	0.36	0.24	0.41	0.19
350	0.62	0.40	0.21	0.47	0.15
400	0.65	0.48	0.17	0.53	0.12

Algorithm 3 is the finite element method. Algorithm 4 is the finite element method combined with the gradient recovery technique

Table 13 Number of external iterations and the CPU time (s) for Algorithms 3 and 4 at CsCl concentration 0.02 M and different voltage (mV)

Voltage (mV)	Algorithm 3 iteration number	Algorithm 4 iteration number	Algorithm 3 CPU time	Algorithm 4 CPU time
25	749	131	3102	738
50	1074	131	4467	760
75	1570	132	6822	757
100	1878	132	7735	743
150	1243	133	5124	760
200	730	133	2979	754
250	1251	134	5085	756
300	844	136	3483	769
350	1810	137	8173	792
400	4836	138	19890	769

Algorithm 3 is the finite element method and Algorithm 4 is the finite element method combined with the gradient recovery technique

equations, such as the diffusion coefficient and the dielectric constant in ion channel, are usually unknown and are given by experience. The parameters used in Algorithm 4 to solve the PNP equations are those fitted by the finite element method (i.e., Algorithm 3). These parameters are "designed" for the finite element method under lower voltages (see [28]), and the purpose is to make the errors between the finite element method and the experimental results within a reasonable range. Therefore, the numerical results may cause greater deviations from the experimental results when the same parameters are applied to Algorithms 4, but they are still within a reasonable range. In conclusion, since the parameters used in Algorithm 4 are the empirical parameters which are designed for Algorithm 3 under lower voltages, it is reasonable that the deviation of the results in Algorithm 4 from the experimental results may be larger than that in Algorithm 3.

Table 14 L^2 norm and maximum norm errors between the numerical solutions $p^1_{1,h}$ and $p^2_{1,h}$, which are numerical approximations to the positive ion concentration p^1 by using Algorithms 3 and 4, respectively

Voltage (mv)	$\frac{\|p^1_{1,h}-p^2_{1,h}\|_\infty}{\|p^1_{1,h}\|_\infty}$	$\frac{\|p^1_{1,h}-p^2_{1,h}\|_0}{\|p^1_{1,h}\|_0}$
25	0.9690	0.9214
50	0.9691	0.9175
75	0.9682	0.9117
100	0.9670	0.9058
150	0.9635	0.8939
200	0.9589	0.8822

Table 15 L^2 norm and maximum norm errors between the numerical solutions $p_{2,h}^1$ and $p_{2,h}^2$, which are numerical approximations to the negative ion concentration p^2 by using Algorithms 3 and 4, respectively

Voltage (mv)	$\frac{\|p_{2,h}^1 - p_{2,h}^2\|_\infty}{\|p_{2,h}^1\|_\infty}$	$\frac{\|p_{2,h}^1 - p_{2,h}^2\|_0}{\|p_{2,h}^1\|_0}$
25	0.6550	0.6256
50	0.6586	0.6185
75	0.6620	0.6175
100	0.6646	0.6179
150	0.6674	0.6193
200	0.6668	0.6153

Next, we study the computational efficiency of Algorithm 4 by comparing it with Algorithm 3. We observe the number of external iterations and CPU time at different voltages. Table 13 shows that the number of iterations for Algorithm 4 is about 130, which is much less than that for Algorithm 3. We can also see from Table 13 that the total CPU time for Algorithm 4 is much less than that for Algorithm 3. These results indicate that Algorithm 4 has better computational efficiency than Algorithm 3 and retains similar accuracy. The improvement of the efficiency may due to the superconvergence property of the gradient recovery operator shown in Section 4. In addition, it is shown from Table 13 that the Gummel iteration numbers with Algorithm 4 change little when the voltage changes. The reason may be that the PNP equations describing the GA ion channel have good properties within the calculated voltage ranges, which leads to the Gummel iteration being insensitive to voltages. Similar phenomena can be observed from Table 2 in [37]. For some complex ion channels, the Gummel iteration numbers may be affected by voltages.

At last, Table 14, 15, and 16 show the L^2 norm and maximum norm errors between the numerical solutions of Algorithms 3 and 4 respectively. It is observed from Tables 14, 15, and 16 that the solution of Algorithm 4 is not so close to that of Algorithm 3. Considering the error between the current simulated by Algorithm 4 and the experimental data is close to that by Algorithm 3 (see Table 12), it is very likely that the exact solution lies between (maybe in the middle of) the two numerical solutions, which leads to the gap of the numerical solutions by using Algorithms 3 and 4.

Table 16 L^2 norm and maximum norm errors between the numerical solutions ϕ_h^1 and ϕ_h^2, which are numerical approximations to the electrostatic potential ϕ by using Algorithms 3 and 4, respectively

Voltage (mv)	$\frac{\|\phi_h^1 - \phi_h^2\|_\infty}{\|\phi_h^1\|_\infty}$	$\frac{\|\phi_h^1 - \phi_h^2\|_0}{\|\phi_h^1\|_0}$
25	0.6105	0.7333
50	0.6003	0.6872
75	0.5603	0.5458
100	0.4891	0.4065
150	0.2708	0.2191
200	0.1620	0.1237

7 Conclusion

In this paper, we first give error estimates in H^1 norms for the finite element approximation to the nonlinear PNP equations. Then the superconvergence analysis is presented for this nonlinear model by using the gradient recovery technique. Numerical experiments verify the theoretical results and show that the gradient of the finite element solution can be improved by using the gradient recovery technique. The superconvergence results are successfully applied to improve the efficiency of the external iteration in the computation of a practical ion channel problem. It is promising to extend this approach to more general settings, such as time-dependent PNP equations for ion channels, PNP equations for semiconductor devices, and modified PNP equations with size effects.

Note that the gradient recovery method used in the paper is a kind of SPR method. The PPR method is also a standard gradient recovery method which can be considered for PNP equations, since it has higher accuracy in some cases such as the linear element under the chevron pattern, and the quadratic element under the regular pattern at element edge centers. The application of the PPR to the PNP practical problems needs further study.

Acknowledgments The authors would like to thank Dr. Minxin Chen and Dr. Shixin Xu for their valuable discussions on numerical experiments.

Funding Y. Yang was supported by the National Natural Science Foundation of China (Nos. 11561016, 11701119, 11771105), the Guangxi Natural Science Foundation (2020GXNSFAA159098, 2017GXNSFFA198012), the Guangxi Colleges and Universities Key Laboratory of Data Analysis and Computation open project fund, and the Hunan Key Laboratory for Computation and Simulation in Science and Engineering, Xiangtan University. C. Liu was partially supported by NSF grant # 1759535 and the United States - Israel Binational Science Foundation (BSF) # 2024246. B. Z. Lu was supported by the National Key Research and Development Program of China (2016YFB0201304), the Science Challenge Program (No. TZ2016003), and the National Natural Science Foundation of China (No. 11771435). L. Q. Zhong was supported by the National Natural Science Foundation of China (Nos. 11671159, 12071160), the Guangdong Basic and Applied Basic Research Foundation (No. 2019A1515010724), the Characteristic Innovation Projects of Guangdong Colleges and Universities, China (No. 2018KTSCX044), and the General Project topic of Science and Technology in Guangzhou, China (No. 201904010117).

References

1. Adams, R.A.: Sobolev Spaces. Academic Press, New York (1975)
2. Andersen, O.S.: Ion movement through gramicidin a channels interfacial polarization effects on single-channel current measurements. Biophys. J. **41**(2), 135–146 (1983)
3. Brandts, J., KŘÍŽEK, M.: Gradient superconvergence on uniform simplicial partitions of polytopes. IMA J. Numer. Anal. **23**(3), 489–505 (2003)
4. Babuška, I., Strouboulis, T., Upadhyay, C.S., Gangaraj, S.K., Copps, K.: Validation of a posteriori error estimators by numerical approach. Int. J. Numer. Meth. Eng. **37**(7), 1073–1123 (1994)
5. Bank, R.E., Xu, J.: Asymptotically exact a posteriori error estimators, Part i: Grids with superconvergence. SIAM J. Numer. Anal. **41**(6), 2294–2312 (2003)
6. Brenner, S.C., Scott, L.R.: The Mathematical Theory of Finite Element Methods. Springer, New York (1994)
7. Cao, W.M.: Superconvergence analysis of the linear finite element method and a gradient recovery postprocessing on anisotropic meshes. Math. Comput. **84**(291), 89–117 (2015)

8. Cardenas, A.E., Coalson, R.D., Kurnikova, M.G.: Three-dimensional Poisson-Nernst-Planck theory studies: influence of membrane electrostatics on gramicidin a channel conductance. Biophys. J. **79**(1), 80–93 (2000)
9. Carstensen, C., Bartels, S.: Each averaging technique yields reliable a posteriori error control in FEM on unstructured grids. i: low order conforming, nonconforming, and mixed FEM. Math. Comput. **71**(239), 945–969 (2002)
10. Chen, C.M.: Superconvergence and extrapolation of the finite element approximations to quasilinear elliptic problems. Northeastern Math. J. **2**, 228–236 (1986)
11. Chen, J., Wang, D., Du, Q.: Linear finite element superconvergence on simplicial meshes. Math. Comp. **83**, 2161–2185 (2014)
12. Chen, L.: Superconvergence of tetrahedral linear finite elements. Int. J. Numer. Anal. Model. **3**(3), 273–282 (2006)
13. Chen, M., Lu, B.Z.: TMSMesh: a robust method for molecular surface mesh generation using a trace technique. J. Chem. Theory Comput. **7**(1), 203–212 (2011)
14. Chen, Y., Wu, L.: Second-Order Elliptic Equations and Elliptic Systems. Science Press, Beijing (1991). (in Chinese)
15. Cohen, H., Cooley, J.W.: The numerical solution of the time-dependent Nernst-Planck equations. Biophys. J. **5**(2), 145–162 (1965)
16. Du, L., Yan, N.N.: Gradient recovery type a posteriori error estimate for finite element approximation on non-uniform meshes. Adv. Comput. Math. **14**(2), 175–193 (2001)
17. Gao, H.D., He, D.D.: Linearized conservative finite element methods for the Nernst-Planck-Poisson equations. J Sci. Comput. **72**(3), 1269–1289 (2017)
18. Gummel, H.K.: A self-consistent iterative scheme for one-dimensional steady state transistor calculations. IEEE T. Electron Dev. **11**(10), 455–465 (1964)
19. Guo, H.L., Yang, X.: Gradient recovery for elliptic interface problem: i. body-fitted mesh. Commun. Comput. Phys. **23**(5), 1488–1511 (2018)
20. Guo, H.L., Xie, C., Zhao, R.: Superconvergent gradient recovery for virtual element methods. Math. Models Methods Appl. Sci. **29**(11), 2007–2031 (2019)
21. Hille, B. Ion Channels of Excitable Membranes, 3rd edn. Sinauer Associates, Sunderland (2001)
22. Horng, T.L., Lin, T.C., Liu, C., Eisenberg, B.: PNP Equations with steric effects: a model of ion flow through channels. J. Phys. Chem. B. **116**(37), 11422–11441 (2012)
23. Hyon, Y.K., Eisenberg, B., Liu, C.: An energetic variational approach to ion channel dynamics. Math. Method. Appl. Sci. **37**(7), 952–961 (2014)
24. Jerome, J.W., Brosowski, B.: Evolution systems in semiconductor device modeling: a cyclic uncoupled line analysis for the gummel map. Math. Method. Appl. Sci. **9**(1), 455–492 (1987)
25. Li, B., Zhang, Z.: Analysis of a class of superconvergence patch recovery techniques for linear and bilinear finite elements. Numer. Meth. Part. D. E. **15**(2), 151–167 (1999)
26. Li, J., Ying, J.Y., Lu, B.Z.: A flux-jump preserved gradient recovery technique for accurately predicting the electrostatic field of an immersed biomolecule. J. Comput. Phys. **396**, 193–208 (2019)
27. Liu, J.H., Jia, Y.S.: Pointwise superconvergence patch recovery for the gradient of the linear tetrahedral element. J. Comput. Anal. Appl. **16**(1), 455–460 (2014)
28. Lu, B.Z., Holst, M.J., McCammon, J.A., Zhou, Y.C.: Poisson-nernst-planck equations for simulating biomolecular diffusion-reaction processes i: finite element solutions. J. Comput. Phys. **229**(19), 6979–6994 (2010)
29. Lu, B.Z., Zhou, Y.C.: Poisson-Nernst-Planck equations for simulating biomolecular diffusion-reaction processes ii: size effects on ionic distributions and diffusion-reaction rates. Biophys. J. **100**(10), 2475–2485 (2011)
30. Lu, B.Z., Zhou, Y.C., Huber, G.A., Bond, S.D., Holst, M.J., McCammon, J.A.: Electrodiffusion: a continuum modeling framework for biomolecular systems with realistic spatiotemporal resolution. J. Chem. Phys. **127**(13), 135102 (2007)
31. Mathur, S.R., Murthy, J.Y.: A multigrid method for the Poisson-Nernst-Planck equations. Int. J. Heat Mass Tran. **52**(17-18), 4031–4039 (2009)
32. Naga, A., Zhang, Z.: A posteriori error estimates based on the polynomial preserving recovery. SIAM J. Numer. Anal. **42**(4), 1780–1800 (2004)
33. Prohl, A., Schmuck, M.: Convergent discretizations for the Nernst-Planck-Poisson system. Numer. Math. **111**(4), 591–630 (2009)
34. Shen, R.G., Shu, S., Yang, Y., Lu, B.Z.: A decoupling two-grid method for the time-dependent Poisson-Nernst-Planck equations. Numer. Algo. https://doi.org/10.1007/s11075-019-00744-4 (2019)

35. Shi, D.Y., Yang, H.J.: Superconvergence analysis of finite element method for Poisson-Nernst-Planck equations. Numer. Meth. Part. D. E. **35**, 1206–1223 (2019)
36. Sun, Y.Z., Sun, P.T., Zheng, B., Lin, G.: Error analysis of finite element method for Poisson-Nernst-Planck equations. J. Comput. Appl. Math. **301**, 28–43 (2016)
37. Tu, B., Chen, M.X., Xie, Y., Zhang, L.B., Eisenber, B., Lu, B.Z.: A parallel finite element simulator for ion transport through three-dimensional ion channel systems. J. Comput. Chem. **34**(24), 2065–2078 (2013)
38. Wu, J., Srinivasan, V., Xu, J., Wang, C.: Newton-krylov-multigrid algorithms for battery simulation. J. Electrochem. Soc. **149**(10), 1342–1348 (2002)
39. Xu, J.: Two-grid discretization techniques for linear and nonlinear PDE. SIAM J. Numer. Anal. **33**(5), 1759–1777 (1996)
40. Xu, J., Zhou, A.: Local and parallel finite element algorithms based on two-grid discretizations for nonlinear problems. Adv. Comput. Math. **14**(4), 293–327 (2001)
41. Yan, N., Zhou, A.: Gradient recovery type a posteriori error estimates for finite element approximations on irregular meshes. Comput. Method. Appl. M. **190**(32-33), 4289–4299 (2001)
42. Yang, Y., Lu, B.Z.: An error analysis for the finite element approximation to the steady-state Poisson-Nernst-Planck equations. Adv. Appl. Math. Mech. **5**(1), 113–130 (2013)
43. Yang, Y., Zhou, A.: Local averaging based a posteriori finite element error control for quasilinear elliptic problems with application to electrical potential computation. Comput. Method. Appl. M. **196**(1-3), 452–465 (2006)
44. Zienkiewicz, O.C., Zhu, J.Z.: The superconvergence patch recovery and a posteriori error estimates. Int. J. Numer. Meth. Eng. **33**(7), 1331–1364 (1992)
45. Zhang, Z.M., Naga: A new finite element gradient recovery method: superconvergence property. SIAM J. Sci. Comput. **26**, 1192–1213 (2005)
46. Zhu, Q., Lin, Q.: Superconvergence Theory of Finite Element Methods. Hunan Science Press, Changsha (1989). (in Chinese)

Affiliations

Ying Yang[1] · Ming Tang[2] · Chun Liu[3] · Benzhuo Lu[4] · Liuqiang Zhong[2]

Ying Yang
yangying@lsec.cc.ac.cn

Ming Tang
mingtang@m.scnu.edu.cn

Chun Liu
cliu124@iit.edu

Benzhuo Lu
bzlu@lsec.cc.ac.cn

[1] School of Mathematics and Computational Science, Guangxi Colleges and Universities Key Laboratory of Data Analysis and Computation, Guilin University of Electronic Technology, Guilin, 541004, Guangxi, People's Republic of China

[2] School of Mathematical Sciences, South China Normal University, Guangzhou, 510631, People's Republic of China

[3] Department of Applied Mathematics, Illinois Institute of Technology, Chicago, USA

[4] LSEC, the National Center for Mathematics and Interdisciplinary Sciences, Academy of Mathematics and Systems Science, Chinese Academy of Sciences, Beijing, 100190, People's Republic of China